A&A 409, 147–158 (2003)
DOI: 10.1051/0004-6361:20030973
© ESO 2003

Astronomy & Astrophysics

Constraints on the IMF and the brown dwarf population of the young cluster IC 348⋆,⋆⋆

T. Preibisch[1], T. Stanke[1], and H. Zinnecker[2]

[1] Max-Planck-Institut für Radioastronomie, Auf dem Hügel 69, 53121 Bonn, Germany
[2] Astrophysikalisches Institut Potsdam, An der Sternwarte 16, 14482 Potsdam, Germany

Received 28 January 2003 / Accepted 10 June 2003

Abstract. We use a deep near-infrared census of the young stellar cluster IC 348 to construct and analyze its luminosity function. Our mosaic image of IC 348 covers the full extent of the cluster with a completeness limit of $J \sim 19.5$ and is therefore sensitive for 2 Myr old cluster members with masses as low as $M \geq 0.005\,M_{\odot}$ for the mean extinction of the known cluster members ($A_V \sim 3.5$ mag). By using information on stellar ages, extinctions, and the binary population in IC 348 from several recent studies, we can derive statistical constraints on the stellar and sub-stellar mass function of the cluster by modeling the observed luminosity function. We find that the stellar part of the mass function in IC 348 is well described by the galactic field star IMF. While several brown dwarfs have recently been identified in IC 348, our data show that the cluster harbors only a relatively small population of sub-stellar objects. We find that brown dwarfs in the mass range 0.02–0.075 $M_{\odot}$ constitute at most ∼10% of the total cluster population, in contrast to recent results suggesting much larger brown dwarf populations in other young clusters and also the galactic field. Our results suggest that IC 348 has ∼2× fewer brown dwarfs than the Orion Trapezium cluster. A similar brown dwarf "deficit" was recently found in the Taurus star forming region. We speculate about the possible causes for this result, including the presence or absence of nearby massive stars and their influence on the formation of low-mass young stellar objects.

Key words. stars: pre-main sequence – stars: low-mass, brown dwarfs – stars: luminosity function, mass function – open clusters and associations: general

1. Introduction

The initial mass function (IMF) is of utmost importance for any theory of star formation. While the theoretical expectation is that the IMF should vary systematically with the star formation environment, no really convincing evidence for variations in the stellar part of the IMF has yet been found (for recent reviews see Kroupa 2001, 2002; Scalo 1998). The effects of environment may be clearest at the low-mass end of the IMF, as one might imagine that the least massive protostars are most strongly affected by external effects. The sub-stellar part (<0.075 $M_{\odot}$) of the IMF, which is not as well characterized as the stellar mass function, is therefore a good point to look for variations in different environments.

After the first detection of BDs (see Rebolo et al. 1995; Oppenheimer et al. 1995) numerous sub-stellar objects have been found in (young) clusters and also in the galactic field (for an overview see Oppenheimer et al. 2000 or the proceedings of the IAU Symp. 211 on Brown Dwarfs; Martin 2003). During the last couple of years, important steps in the characterization of the sub-stellar mass function have been made (e.g. Reid 1999). In a summary of recent results Chabrier (2002) concluded that the total number of BDs (in the mass range 0.001–0.07 $M_{\odot}$) in the Galactic disk is similar to the number of stars.

IC 348 is a very young cluster located in the Perseus molecular cloud complex at a distance of about 310 pc (cf. Herbig 1998). For a long time, the cluster was believed to consist of just a dozen T Tauri members (Herbig 1954, Harris et al. 1954), but recent sensitive optical (Herbig 1998), near-infrared (Lada & Lada 1995; Luhman et al. 1998), and X-ray observations (Preibisch et al. 1996; Preibisch & Zinnecker 2001, 2002) have shown that IC 348 contains more than 100 stars. Luhman et al. (1998) showed that the mass spectrum in IC 348 extends well into the sub-stellar regime. In a deep near-infrared spectroscopic survey of faint objects in IC 348, which later was extended by Luhman (1999), at least 8 objects could be identified which appear to have masses below 0.075 $M_{\odot}$, i.e. the hydrogen-burning mass-limit.

Send offprint requests to: T. Preibisch,
e-mail: preib@mpifr-bonn.mpg.de

⋆ Based on observations obtained at the German-Spanish Astronomical Centre, Calar Alto, operated by the Max-Planck-Institute for Astronomy, Heidelberg, jointly with the Spanish National Commission for Astronomy.

⋆⋆ Table 1 is only available in electronic form at http://www.edpsciences.org

Article published by EDP Sciences and available at http://www.aanda.org or http://dx.doi.org/10.1051/0004-6361:20030973

Najita et al. (2000) [N00 hereafter] identified further brown-dwarf candidates by deep HST/NICMOS narrow-band imaging, using the 1.9 μm water absorption band strength as an indicator of spectral type. Their observations covered the $5' \times 5'$ core of IC 348, are complete down to masses of $\sim 0.02\,M_\odot$, and revealed 20–30 substellar candidates. Liu (2002) performed K-band spectroscopy for some of the BD candidates in IC 348 at the Subaru 8 m Telescope and found that for the faintest objects only marginally useful spectra can be obtained. This demonstrates that a spectroscopic identification of the *full* population of BDs, down to the deuterium burning mass limit at $0.015\,M_\odot$ and across the whole cluster area, would require a large amount of observing time. The existing samples of spectroscopically identified BDs are necessarily subject to the problems of small number statistics.

On the other hand, near-infrared photometric observations of a compact cluster like IC 348 can rather easily go deep enough to detect *all* cluster members down to masses below $\sim 0.01\,M_\odot$. It is thus relatively easy to determine the full cluster luminosity function. Modeling of the observed luminosity function (cf. Zinnecker et al. 1993) then allows one to obtain statistical constraints on the mass function. An early attempt to gain information about the low-mass and sub-stellar IMF on the basis of an observed luminosity function was presented by McCaughrean et al. (1995) for the case of the Trapezium cluster.

In general, the knowledge of the luminosity function is not sufficient to draw strong conclusions on the underlying mass function, because the individual stellar magnitudes are not only a function of the stellar mass, but also strongly depend on the stellar age and the extinction. If, however, the distribution of stellar ages and extinctions is known as a piece of independent information, this ambiguity is largely removed and the luminosity function basically depends only on the mass function. Although it is clear that any luminosity function modeling procedure can give only statistical constraints on the mass function, i.e. yields less information than a (spectroscopic) one-by-one identification of cluster members, it allows nevertheless important insights with a relatively small observational effort.

While many similar studies of cluster luminosity functions (e.g. Zinnecker et al. 1993; Lada et al. 1998) have been performed in the K-band (2.2 μm), we have chosen the J-band (1.2 μm) for our study of IC 348. Our choice was motivated by the fact that the J-band flux seems to be a better tracer of the stellar bolometric luminosity (cf. Kenyon & Hartmann 1995). This is even more important as we are dealing with very young stars, for which the K-band flux is often strongly affected by excess emission due to hot circumstellar material, most pronounced in the case of the classical T Tauri stars. In the J-band, this excess emission is much reduced. The K-band has the advantage of being less sensitive to extinction than the J-band ($A_K \approx 0.11 \times A_V$; $A_J \approx 0.28 \times A_V$; cf. Rieke & Lebofsky 1985), but this is not very relevant for our particular study, since the extinction of the stars in IC 348 is not very large ($A_J \lesssim 3$ mag; see below).

For the distance of IC 348 we adopt here a value of 310 pc (see H98 for a detailed justification of this value). We note that IC 348 is associated to the Per OB2 association, and the distance we use is in very good agreement with the recent determination of Per OB2 distance (318 ± 27 pc; de Zeeuw et al. 1999) based on a detailed analysis of the Hipparcos data. Also, the recent detection of δ Scuti-like pulsations in one of the F-type stars in IC 348 by Ripepi et al. (2002) allowed an independent distance determination that is in full agreement with our assumption of 310 pc and rules out earlier suggested values of only about 250 pc (e.g. Cernis 1993).

2. Deep *J*-band imaging of IC 348

2.1. Observations and data reduction

The observations discussed in this paper were obtained during the night of 2nd Dec. 2001 using the Omega Prime wide-field near-infrared camera (Bizenberger et al. 1998) on the Calar Alto 3.5 m telescope in service observing mode. The camera uses a 1024 × 1024 pixel HgCdTe array and provides a $6.7' \times 6.7'$ field-of-view at a pixel scale of $0.4''$. The images were taken through a standard J-band filter (1.13–1.42 μm). We obtained a 3×3 mosaic image covering an $18' \times 18'$ area around IC 348. Furthermore, we also obtained two background images about $30'$ east and west of IC 348, each covering a $6' \times 12'$ area. The stepsize between the mosaic positions was chosen such that a significant overlap between the frames allowed accurate registration of the images relative to each other. At each mosaic position, a sequence of 15 images with individual exposure time of 20 s was repeated in 5 dither positions with offsets of about $20''$. The final per pixel integration time is thus $5 \times 15 \times 20\,\mathrm{s} = 1500$ s (25 min). The observing conditions were photometric during the whole night, and the mean seeing was $1.3''$.

The data reduction followed standard infrared procedures. For each individual exposure, sky frames were constructed by median averaging (to remove stellar images) of adjacent (in time and on the sky) exposures. These were then subtracted from the frames, thus also removing the bias level. Bad pixels were masked and excluded from further processing. The frames were then divided by a normalized flat-field, which was constructed of exposures of the dome, once with a flat-field lamp on, then off. Finally, the images were registered and median averaged to reject cosmic ray events. As the edges of the final mosaic constructed from the dithered exposures have not the full integration time, only that part of the mosaic with the full 25 minutes integration time was used for further analysis. This final image measures $18.6' \times 18.4'$, giving a field of view of ~340 square-arcminutes. The center of our final image is at the position RA = $3^{\mathrm{h}}44^{\mathrm{m}}30^{\mathrm{s}}$, Dec = $32^\circ 08' 00''$ (J2000). The sky fields both measured about 72 square-arcmin. The UKIRT faint infrared standard star FS 113 was observed for photometric calibration.

2.2. Photometry

The MIDAS INVENTORY package was used for the source detection, and the resulting source list carefully checked for apparent misidentifications such as multiple detections of strongly saturated sources, wrong source detections in

diffraction spikes of bright sources, extended, nebulous features, and the H_2 features associated with the outflows in the HH211 region. 1991 sources were thus found on the cluster mosaic, and 632 and 662 sources were found in the comparison fields. Aperture photometry was then done using the DAOPHOT package, dealing separately with the subfields of the cluster mosaic and the comparison fields. This was done in order to correct the photometry for the actual atmospheric extinction and to allow for apertures varying as the actual seeing. Thereafter the photometry was carefully checked for possible cloud contamination by first comparing brightness measurements for the individual exposures taken on each subfield, and then comparing brightness measurements for stars in the overlap region between the subfields. We did not find any evidence for intervening clouds, with the brightness measurements scattering only little (typically 0.02 mag for reasonably bright stars) around the mean value. We thus regard the data to be taken under photometric conditions.

The photometry was also compared with the 2MASS data. Again, there was a very good correspondence between the two data sets, although there is a small offset between the two (2MASS yields about 0.05–0.1 mag fainter stars; note however that our measurements do not show any significant offset from the photometry obtained by Lada & Lada 1995). This indicates that the uncertainty of the absolute calibration of our data is 0.1 mag or less. Furthermore, the comparison between 2MASS and our photometry suggests that our data suffer from saturation for stars brighter than about $J \sim 12$. Thus for stars brighter than $J = 12.5$ the photometry from 2MASS was used instead of our own measurements. The comparison of brightness measurements obtained from the individual exposures suggests that measurement errors are less than 0.1 mag for stars as faint as $J \sim 18{-}18.5$.

The limiting magnitude of the exposures was found to be at $J \sim 21$. The number of stars per magnitude closely follows a power-law. The completeness limit of our images can be approximated as the magnitude at which the distribution starts to deviate from a power-law relation, which we find at $J_{\mathrm{compl.}} = 19.5$. A similar result was also found by adding artificial stars to the images and applying the same detection techniques as described above. Comparing this with the expected magnitudes of 2 Myr old BDs (B98; Baraffe et al. 2003) at the distance of IC 348, we conclude that our data are complete to all BDs with masses of $0.005\,M_\odot$ or more for the typical extinction of the known cluster members ($A_V \sim 3.5$ mag) and to objects with masses of $0.02\,M_\odot$ or more for extinctions of up to $A_V = 11$ mag.

The BDs identified by Luhman (1999) are clearly visible in our data and are marked in Fig. 1. A table containing the positions and magnitudes of all stars detected in our image is given in Table 1 (available in electronic form only).

Table 1. *J*-band magnitudes of the sources detected in our IC 348 image. The source names contain the J2000 coorinates. The complete version of this table is in electronic form. The printed edition contains only a sample.

IC348-J	*J* [mag]
034350.6+321059	18.69
034350.6+321231	19.46
034350.7+321306	14.20
034350.7+321125	19.98
034350.8+321433	19.65
...	...
...	...
...	...

3. Determination of the cluster luminosity function

3.1. Definition of the cluster area

The first step in the determination of the *J*-band luminosity function (JLF) of IC 348 is the definition of the cluster area. The spatial distribution of objects in our mosaic image shows an excess in the surface density of objects up to radii of 5′–6′ from the cluster center; this is in good agreement with the results of H98 and of Lada & Lada (1995). We therefore use a cluster radius of 6′ for the following analysis.

3.2. Magnitude distributions in the cluster and background fields

We constructed histograms of the *J*-band magnitudes of all point sources located in the cluster area and the background areas; these histograms are shown in Fig. 2. The cluster area contains 762 objects, the two background areas contain 1294 objects.

The number of objects per magnitude interval in the background fields closely follows a power-law, as expected for a uniformly distributed background population. The cluster field histogram also shows a power-law like increase in the number of objects for faint magnitudes ($J \gtrsim 16$), but in the magnitude range $J \sim 10{-}16$ the distribution shows a strong bump, which represents the cluster population.

3.3. Background subtraction

In order to properly correct the cluster area histogram for the background population in the cluster field, we need a model for the distribution of background objects in the cluster area. To construct this background model, we scaled the background magnitude histogram according to the areas covered by our cluster field and the background fields. Furthermore, we also have to take into account the difference in interstellar extinction along the line-of-sight (LOS) to the background fields as compared to the LOS in the direction of IC 348. What we need to determine is the amount of additional extinction along the IC 348 LOS **in excess** of the background field LOS extinction.

IC 348 is located at the eastern edge of the Perseus molecular cloud complex. A dense cloud core about 10′ to the southwest of the cluster center contains several deeply embedded infrared sources with extinctions exceeding ∼20 mag in A_V as well as the very young molecular hydrogen jet HH 211 (McCaughrean et al. 1994) and the IC 348 MMS outflow

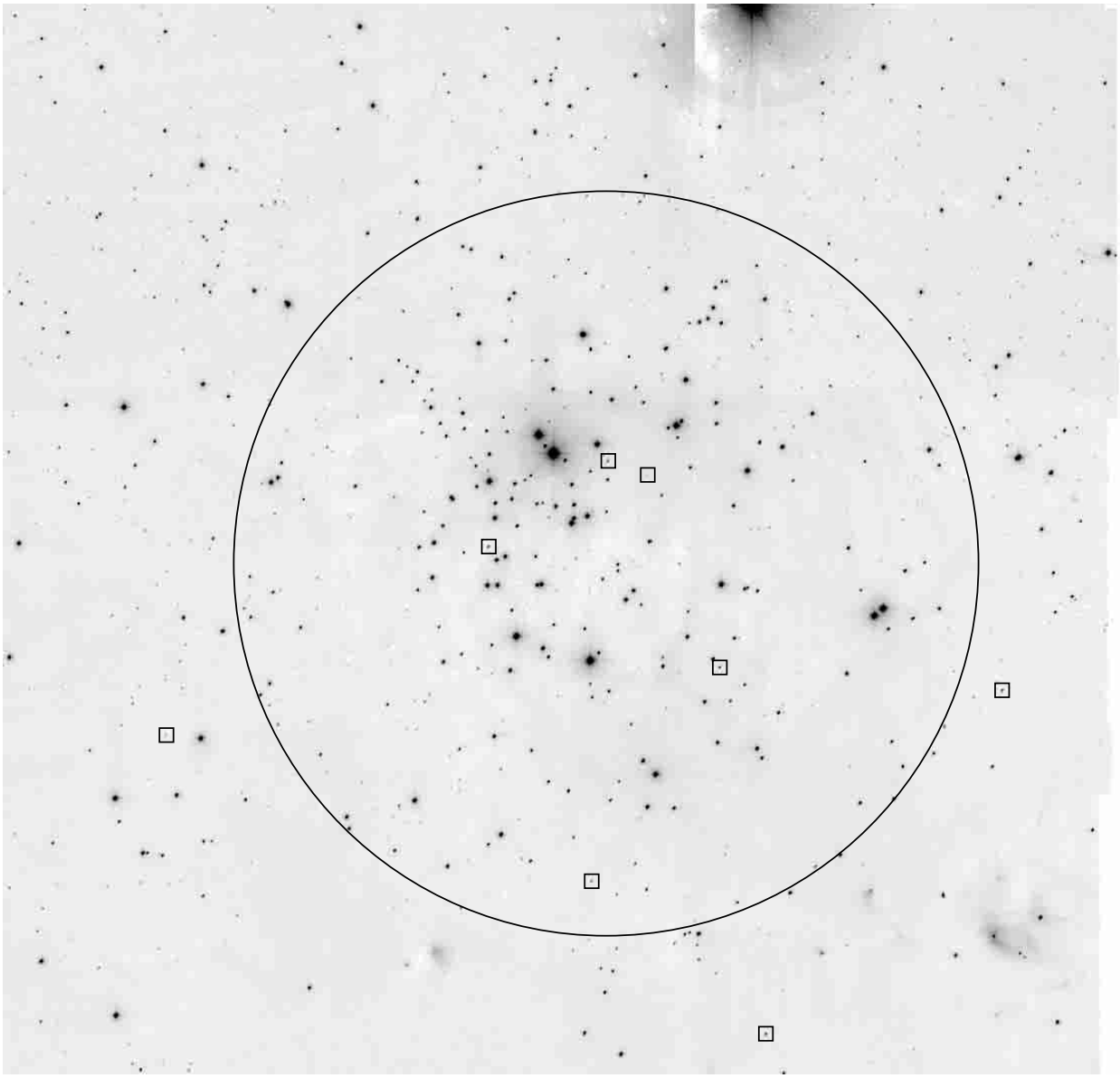

Fig. 1. Our J-band mosaic image of IC 348, showing a $18.6' \times 18.4'$ field with a square-root intensity scale. The eight BDs (objects with spectral types ≥M 6.5) identified by Luhman (1999) are marked by boxes. The large circle marks the cluster area.

(Eislöffel et al. 2003). In the central cluster area, however, the cloud extinction is much lower. Cernis (1993) found that the whole region is covered by a foreground layer of diffuse extinction with $A_V \sim 0.7$ mag, in good agreement with the results obtained earlier by Cernicharo et al. (1985). Both studies also found a second layer of absorbing material, the dark clouds in the Perseus complex, producing extinctions of several magnitudes.

A quantitative estimate of the extinction caused by the IC 348 cloud can be based on the extinctions derived for some 50 background stars in the central cluster area by N00, which show a broad distribution from $A_V \sim 1$ mag up to $A_V \sim 10-12$ mag.

For the extinction in the direction of our two background fields, we can use the reddening maps of Schlegel et al. (1998), which suggest extinctions between $A_V \lesssim 2$ mag and $A_V \sim 6.5$ mag. Given these results, we have to add ∼4 mag of extinction to the background data to correct for this difference. This corresponds to $\Delta A_J = 1.1$ mag.

3.4. The cluster JLF

The cluster JLF can now be determined by subtracting the reddened background histogram from the cluster field histogram. The resulting cluster JLF can be seen in Fig. 3. The most important features of the cluster JLF are a pronounced peak at $J \sim 13.5$ and the strong drop in the range $J \sim 14-16$. The histogram shows a number of objects in the $J \sim 17.5-19.5$ range, but this is not significant and can be fully explained as a statistical fluctuation of the background subtraction. In the following plots we therefore show these insignificant histogram bins only by thin dotted lines.

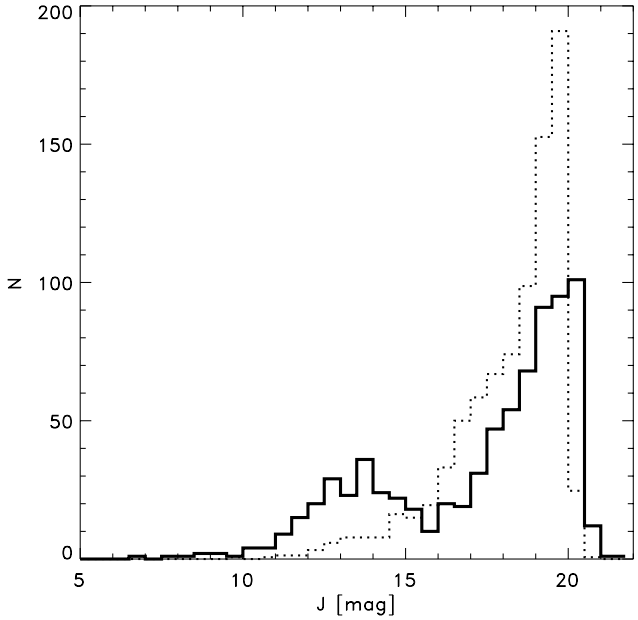

Fig. 2. Histogram of J-band magnitudes for the central 6′ radius area in our IC 348 cluster image (thick solid line) compared to the histogram for the background fields (dotted line, scaled to the same area as the cluster region).

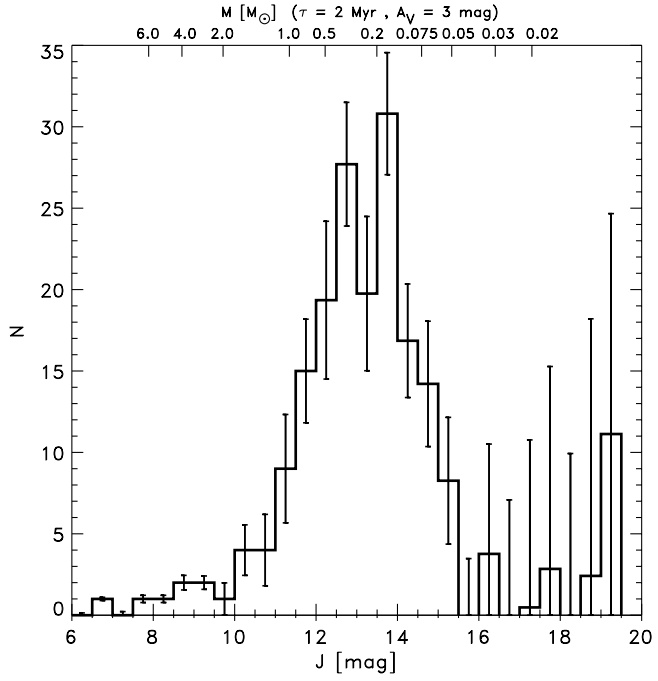

Fig. 3. JLF of IC 348, computed by subtracting the background model histogram from the cluster area histogram. The error bars represent the uncertainties caused by the photometric errors ($\sigma \sim 0.05$ mag) and the Poisson statistical uncertainties of the background subtraction.

4. JLF modeling procedure

We performed detailed simulations to model the observed JLF of IC 348. The general outline of our Monte-Carlo simulation procedure is as follows: In the first step, we randomly draw 30 000 stellar masses from a distribution specified by the input IMF. For each simulated star we draw a value for the stellar age from the age distribution described below. Then the J-band magnitude of each simulated star is determined according to its mass and age using pre-main sequence (PMS) evolutionary models. Finally, each star is extincted by randomly drawing a value for A_V from the distribution described below.

4.1. Mass function

In this paper we will mainly use power-law functions to describe the mass function:

$$\Psi(M) = \frac{\mathrm{d}N}{\mathrm{d}M} = c\, M^{\alpha} \qquad \text{for} \qquad M_{\min} \le M \le M_{\max},$$

where $\Psi(M)$ gives the number of stars per unit mass. We note that some authors prefer to use the number of stars per unit log mass, $\xi(M) = \frac{\mathrm{d}N}{\mathrm{d}\log M}$, and that $\Psi(M) \propto M^{\alpha}$ corresponds to $\xi(M) \propto M^{\alpha+1}$.

4.2. Stellar ages

The ages derived for individual stars by H98 and L98 by comparison with PMS model isochrones range from less than 1 Myr to about 10 Myr, with the majority of the objects having ages of a few Myr (a mean age of ∼1.3 Myr was derived by H98). It is important to note that the ages determined by comparison with PMS model isochrones, which we will denote "isochronal ages", are not identical to the true ages of the objects. The apparent age spread derived from individual isochronal ages is always larger than the true age spread, because any measurement errors and the intrinsic variability of the young stars will increase the apparent spread in the isochronal ages. Another important factor are unresolved binary systems, which will lead to systematically overestimated luminosities which in turn transform into too young isochronal ages. In summary, the true mean age of a stellar population will be somewhat larger than the mean of the isochronal ages, and the true age spread will always be smaller than the scatter of the isochronal ages. A detailed analysis of these effects can be found in Preibisch & Zinnecker (1999).

We consider both effects in our simulations as follows. In our Monte-Carlo programs we draw ages from a Gaussian distribution with $\langle \log(\tau) \rangle = 6.3$ and $\sigma_{\log(\tau)} = 0.1$. If an age of less than 0.7 Myr or larger than 7 Myr is drawn, the drawing is repeated. The mean value of the resulting age distribution is 2 Myr; this is consistent with the mean "isochronal age" of ∼1.3 Myr if a binary fraction of ∼50% is assumed. The width of the simulated age distribution is also roughly consistent with the apparent spread of "isochronal ages", if the effect of measurement errors is considered.

4.3. Extinction of the cluster members

The extinctions of the stars in IC 348 derived by H98 and L98 range from $A_V \sim 1$ mag to $A_V \lesssim 10$ mag, with a mean of $A_V \sim 3.5$ mag. The NICMOS study of N00 revealed several stars with somewhat higher extinctions. In our simulations, we randomly draw values for the extinction from a half-Gaussian distribution (i.e. only positive numbers are used) with

a width $\sigma(A_V) = 4$ mag and increase every extinction value by $A_V = 0.7$ mag (to account for the diffuse foreground extinction mentioned above). The corresponding values range from 0.7 mag to ≈20 mag with a mean of 3.9 mag. The resulting distribution is very similar to the empiric distribution found by N00 and also consistent with the results of H98 and L98.

4.4. PMS evolutionary models

We use the recent version of the Baraffe et al. (1998) models (see also Chabrier & Baraffe 2000) which have been found to be very well consistent with observational constraints (cf. Luhman 1999; White et al. 1999). These models have the additional advantage that they give not only the stellar luminosity and effective temperature as a function of mass and age, but also the magnitudes in observational passbands. So there is no need to transform luminosities and effective temperatures to magnitudes and the uncertainties in the calibration of these transformations can be avoided.

The Baraffe et al. models start at an age of 1 Myr and cover masses from 0.02 $M_\odot$ up to 1.2 $M_\odot$. Since IC 348 contains also some stars with higher masses (the most massive member is the B5 star BD +31° 643 with $M \sim 6\,M_\odot$), we used the Palla & Stahler (1999) models for masses above 1.0 $M_\odot$. In the range of ages we need here, these two sets of models agree reasonably well at 1 $M_\odot$. In order to compute the J-band magnitudes of the stars with $M \geq 1.0\,M_\odot$, we use the intrinsic colors and bolometric corrections as a function of effective temperature from the tabulation in Kenyon & Hartmann (1995) and Leggett et al. (1996).

4.5. Unresolved binaries

It is well known that many, perhaps most stars are members of multiple systems. About 50% of the field stars in the solar neighborhood are binaries or higher order multiple systems (cf. Duquennoy & Mayor 1991; Fischer & Marcy 1992). A recent study of the binary population in IC 348 has been performed by Duchene et al. (1999), who conducted a near-infrared adaptive optics survey of 66 members of IC 348 and found 12 binary systems in the separation range 0.1″–8″. They concluded that the binary fraction in IC 348 is consistent with that in the solar neighborhood, i.e. that IC 348 displays *no evidence* for an overabundance of multiple systems. We therefore assume that 50% of the stars in IC 348 are binaries, most of which would be unresolved in our image.

The effects of unresolved binary components are modeled in the following way: To each primary star we randomly add a companion with a probability equal to the assumed binary fraction (50%). The companion mass is drawn from the same IMF as the primary mass, but with the restriction that it must be smaller than the primary mass. For these simulated binary systems we use the combined system magnitude, containing the flux from the primary and the companion, instead of the primary magnitude.

4.6. Fit quality

In order to evaluate how good (or bad) the different model IMFs reproduce the observed cluster JLF, we will compare below the histograms of the cluster JLF to the corresponding histograms computed from the model IMFs. The normalization of the model IMF histograms was chosen so that it reproduces the number of objects in the $J = 10-14$ mag range.

Since we also would like to decide whether a certain model provides a statistically acceptable description of the data and to compare the success of different models in reproducing the observed JLF, we need a quantitative estimate of the "fit quality". While in many similar studies a χ^2 test is used for this purpose, we note that this test is not completely suitable here: it provides a correct estimate for the probability that a specific model is consistent with the observed data only if the errors are normally distributed, which is not the case here. We therefore decided to use a Kolmogorov-Smirnov two-sample test (KS test), which is a non-parametric test and thus yields correct probabilities without conditions for the distribution of the errors. A KS test between the observed cluster JLF (in which we treat the histogram points at $J > 17$ as statistical fluctuations, i.e. assume them to be zero) and the model JLF gives the probability that the deviations between the model and the data are purely caused by statistical fluctuations. For the interpretation of the resulting probabilities we note that a model with $P_{\rm KS} \gtrsim 0.5$ provides a reasonably good description of the data, while a probability of, e.g. $P_{\rm KS} = 0.05$ shows that the model can be rejected at the 95% confidence level and can be considered to be invalid.

In Table 2 we summarize all relevant data for each of the different IMF models considered in this paper: the analytic formula for the mass function $\mathrm{d}N/\mathrm{d}M$, the "fraction of BDs" which we define as the fraction of objects in the mass range 0.02–0.075 $M_\odot$ among all objects computed by integration of the mass function, and finally the KS test probability. A comparison of most of the mass functions considered in this paper is shown in Fig. 8.

4.7. Uncertainties of the modeling

It is clear that the reliability of the modeling results depends on the validity of the assumption on ages, extinctions, binary fractions and the correctness of the employed PMS models. As discussed above, due to the numerous studies of IC 348, we can use relatively well founded and thus reliable assumptions for these factors. In order to see to what extent our results might depend on the use of one specific PMS model, we have also performed some tests with different sets of models. For this we firstly employed the D'Antona & Mazzitelli (1997) models, and secondly also a combination of the Palla & Stahler (1999) models for masses $0.1 \leq M/M_\odot \leq 6$ with the Burrows et al. (1997) models for masses $0.02 < M/M_\odot \leq 0.1$. We found that the use of these models instead of the B98 models generally causes only slight differences in the shapes of the simulated luminosity functions. The IMF power-law slopes α inferred from the fits to the observed luminosity function with the different models do generally not differ by more than ∼0.1.

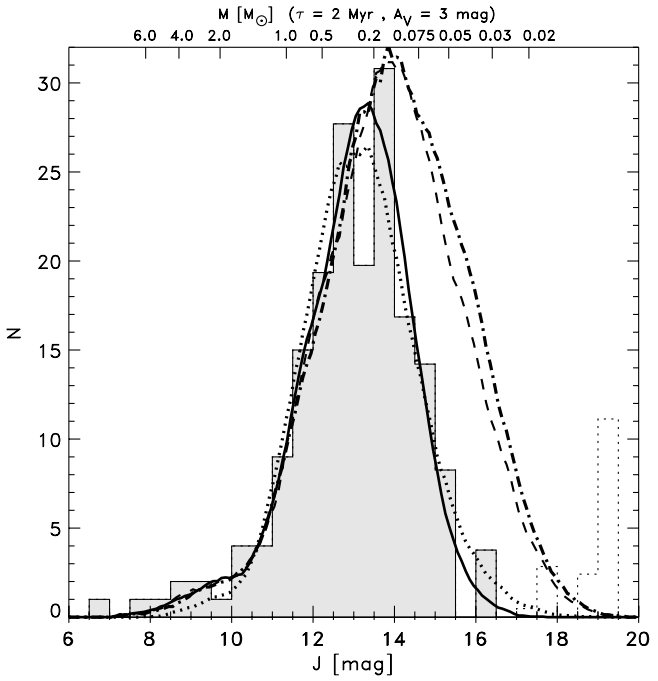

Fig. 4. The IC 348 JLF (histogram) compared to a model based on the Kroupa (2002) field IMF (dashed line), the stellar part of the Kroupa (2002) field IMF (solid line), the Chabrier (2002) log-norm IMF (dashed-dotted line), and our log-norm IMF fit (dotted line).

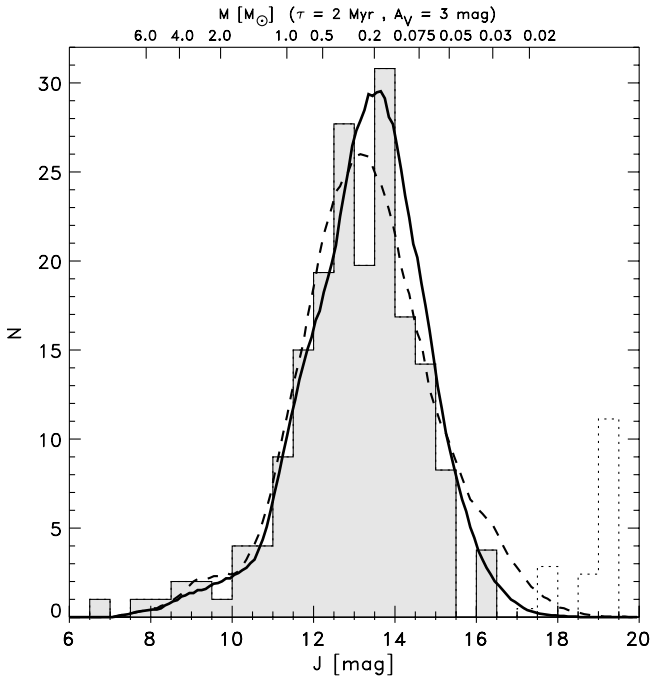

Fig. 5. The IC 348 JLF (histogram) compared to the two marginally acceptable Kroupa IMF like models with maximum BD population. The solid line shows the model with the power-law slope $\alpha = +2.5$ in the sub-stellar part (model "Fit I"), the dashed line shows the model "Fit II", in which the change of the power-law slope occurs at 0.22 $M_\odot$.

Also, the derived sizes of the substellar population are quite similar for the different models. The differences in the IMF determinations with different PMS models are rather small because the luminosities predicted by the different models for PMS objects with ages of a few Myr agree rather well (for a more detailed discussion of these differences see Muench et al. 2002). Therefore, none of our conclusions drawn in this paper depends significantly on the choice of a specific PMS model.

5. JLF modeling

5.1. Comparison with the galactic field IMF

We will start our modeling with recent representations of the galactic field IMF. We first consider the following parameterization for the average galactic field IMF in the solar neighborhood given by Kroupa (2002):

$$\frac{\mathrm{d}N}{\mathrm{d}M} \propto \begin{cases} M^{-0.3} & \text{for } 0.02 < M/M_\odot < 0.08 \\ M^{-1.3} & \text{for } 0.08 < M/M_\odot < 0.5 \\ M^{-2.3} & \text{for } 0.5 < M/M_\odot < 100 \end{cases}$$

or, in the shorter notation we will use in the following text, $\alpha[0.02{-}0.08] = -0.3$, $\alpha[0.08{-}0.5] = -1.3$, $\alpha[0.5{-}100] = -2.3$. The comparison of the cluster JLF with the model based on the Kroupa (2002) IMF is shown in Fig. 4. This mass function obviously predicts much more objects at magnitudes $J > 14$ than observed in IC 348. The disagreement between model and data is highly significant, what is clearly confirmed by the very small KS test probability of $P_{\mathrm{KS}} = 4.12 \times 10^{-10}$. This implies that IC 348 contains a significantly smaller number of BDs than expected from the Kroupa (2002) IMF. As the "fraction of BDs" found by integrating the model IMF is 30% (see Table 2, the actual fraction of BDs in IC 348 must be much smaller than this value.

Next we consider a purely stellar IMF, which is identical to the Kroupa (2002) IMF for masses above 0.08 $M_\odot$ and contains *no BDs*. The corresponding model JLF is compared to our observed JLF in Fig. 4 and can be seen to provide a rather good description of the observed JLF ($P_{\mathrm{KS}} = 0.975$). This good agreement also shows that our above assumptions about the cluster properties are reasonable and provide a consistent description of the data. As closer look reveals that the purely stellar IMF predicts slightly too few objects for $J \geq 15$; this suggests the presence of a small BD population in IC 348 (the existence of which was of course already proven by the spectroscopic identification of a few BDs by N00 and L00).

Chabrier (2002) included the results of recent near-infrared surveys (DENIS, 2MASS, SLOAN DSS) in his determination of the stellar and sub-stellar mass function in the Galactic disk. He proposed several possible representations of the IMF, including a log-normal function. This model assumes a Gaussian distribution in $\log M$ with a peak at 0.1 $M_\odot$ and a width of $\sigma(\log M) = 0.627$ (see Table 1 for details). It yields a model JLF which is very similar to that for the Kroupa (2002) IMF and is not consistent with our JLF for IC 348.

We investigated in which way the parameters of the log-normal distribution have to be changed in order to find a good agreement between the observed cluster JLF and the model. The best fit (i.e. the highest P_{KS} value) is found for a model in which the mass function is given by a Gaussian distribution in $\log M$ with a peak at 0.25 $M_\odot$ and a width of $\sigma(\log M) = 0.4$.

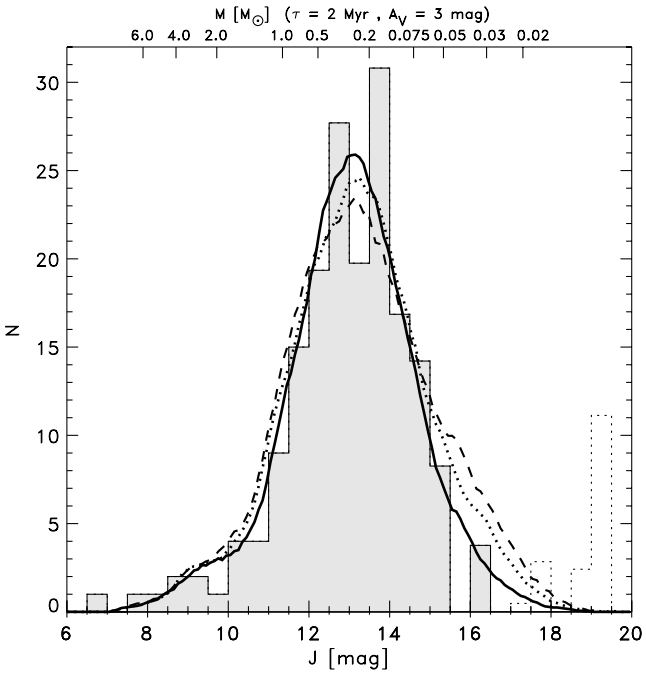

Fig. 6. The IC 348 JLF (histogram) compared to the IMF models for IC 348 derived by Lada et al. (1998); the model L1 is shown by the dashed line, model L2 by the dotted line. The solid line shows the model based on the IMF suggested by Luhman et al. (2000) for IC 348.

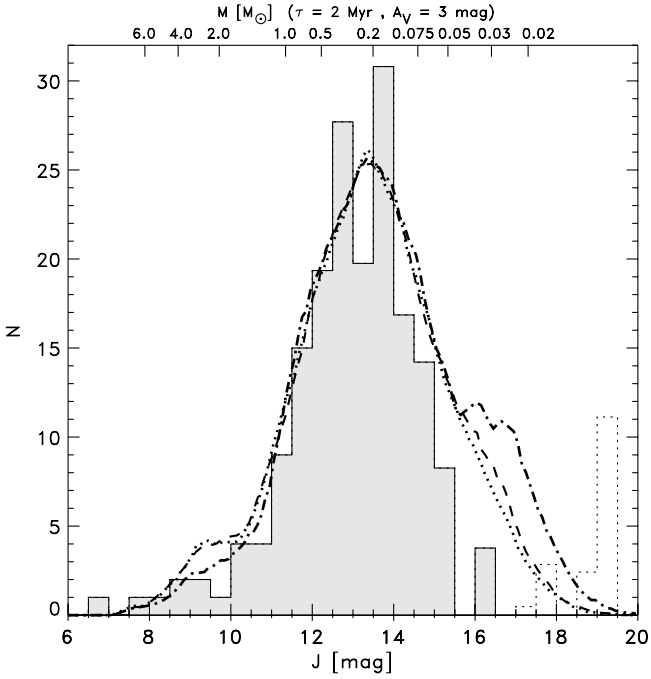

Fig. 7. The IC 348 JLF (histogram) compared to three models for the IMF in the Orion Trapezium Cluster. The dotted line shows the model by Hillenbrand & Carpenter (2000), the dashed line shows the model by Luhman et al. (2000), and the dashed-dotted line the model by Muench et al. (2002).

This model has a BD fraction of 9%, yields $P_{\rm KS} = 0.777$ and is also shown in Fig. 4.

5.2. Constraining the sub-stellar IMF of IC 348

We now want to determine an upper limit to the size the of BD population in IC 348 by considering the following question: How must the Kroupa IMF be changed in order to contain the maximum fraction of BDs that is still marginally consistent (at the 10% level, i.e. $P_{\rm KS} = 0.10$) with the observed JLF? There are two ways in which the Kroupa IMF can be changed: the first possibility is to change the power-law slope in the sub-stellar regime, until the KS test between the model JLF to the observed cluster JLF yields $P_{\rm KS} = 0.1$. We find that the slope must be changed from -0.3 to $+2.5$. The corresponding IMF model (called "Fit I" in Table 2) has a BD fraction of 10% (see Table 1).

The second possibility is to keep the power-law slope fixed at -0.3 and to increase the mass at which the power-law slope changes from -1.3 to -0.3. For this alternative we find that the mass has to be increased from 0.08 $M_\odot$ to 0.22 $M_\odot$ (model "Fit II" in Table 2); the BD fraction of this model is 16%.

Both models are compared to the observed cluster JLF in Fig. 5. This analysis gives an upper limit to the BD fraction of <16% in IC 348.

5.3. Comparison to other IMF determinations for IC 348

Lada et al. (1998) presented a study of the mass function of IC 348 based on the K-band luminosity function (KLF) of the cluster. The completeness limit of their KLF is near $K \sim 14$. Since the typical color of late M-type stars is $J-K \sim 1$, this corresponds to $J \sim 15$, i.e. their data are about 4 mag less deep than our J-band data. In their modeling, they consider two specific models which they find to be consistent with their data. The formulas for both models, called here L1 and L2, are given in Table 2, the model JLFs are compared to the observed cluster JLF in Fig. 6. Model L1 has a BD fraction of 19% and does not provide an acceptable description of our data. Model L2 has a BD fraction of 16% and provides a marginally acceptable fit to the JLF of IC 348. Both models predict more faint objects than observed. The deviations start at $J \sim 15$, i.e. just at the completeness limit of the K-band data used by Lada et al. (1998). We suspect that this explains why these models are consistent with their K-band data but not with our J-band data.

Luhman et al. (2000) determined an IMF for IC 348 based on a spectroscopic sample of cluster members. The simulated JLF based on this model (see Table 1 for details) is also shown in Fig. 6 and yields good agreement with the observed JLF. The model has a BD fraction of 10%.

5.4. IC 348 compared to the Orion Trapezium Cluster

There are several reasons why it is interesting to compare the IMF of IC 348 to that of the Orion Trapezium Cluster. First, this famous star forming region is very well investigated, the stellar population is well known to a high degree of completeness, and several recent studies have tried to derive the IMF of this region. Second, the physical conditions in IC 348 are very different from those in the Trapezium Cluster and this might

Table 2. Summary of model parameters and test statistics for all IMF models considered in this paper. For details see text. $P_{\rm KS}$ values above 0.1, indicating statistically acceptable models, are marked in bold face.

model	mass range [$M_\odot$] / power-law exponent					$P_{\rm KS}$	$\frac{N(0.02-0.075)}{N(>0.02)}$
Kroupa (2002) **galactic field**	[0.02–0.08] $\alpha=-0.3$	[0.08–0.5] $\alpha=-1.3$	[0.5–100.0] $\alpha=-2.3$			4.12×10^{-10}	0.30
Kroupa (2002) **stars only**	[0.08–0.5] $\alpha=-1.3$	[0.5–100.0] $\alpha=-2.3$				**0.97**	0
Chabrier (2002) **galactic field**	peak(M) = 0.1 $M_\odot$, $\sigma(\log M)$ = 0.627					1.80×10^{-12}	0.34
log-norm **fit**	peak(M) = 0.25 $M_\odot$, $\sigma(\log M)$ = 0.4					**0.78**	0.09
maximum BD **Fit I**	[0.02–0.08] $\alpha=+2.5$	[0.08–0.5] $\alpha=-1.3$	[0.5–100.0] $\alpha=-2.3$			*0.10*	0.10
maximum BD **Fit II**	[0.02–0.22] $\alpha=-0.3$	[0.2–0.5] $\alpha=-1.3$	[0.5–100.0] $\alpha=-2.3$			*0.10*	0.16
Lada et al. (1998) **IC 348 (L1)**	[0.02–0.3] $\alpha=-0.6$	[0.3–1.0] $\alpha=-1.4$	[1.0–10] $\alpha=-2.5$			1.26×10^{-2}	0.19
Lada et al. (1998) **IC 348 (L2)**	[0.02–0.2] $\alpha=-0.3$	[0.2–1.0] $\alpha=-1.4$	[1.0–10] $\alpha=-2.5$			**0.11**	0.16
Luhman et al. (2000) **IC 348**	[0.02–0.1] $\alpha=+0.4$	[0.1–0.3] $\alpha=-0.4$	[0.3–2.5] $\alpha=-2.0$	[2.5–10] $\alpha=-2.7$		**0.86**	0.10
Hillenbrand & Carpenter (2000) **Trapezium Cluster**	[0.02–0.15] $\alpha=-0.45$	[0.15–0.4] $\alpha=-1.22$	[0.4–1.0] $\alpha=-1.62$	[1–3] $\alpha=-1.88$	[3–10] $\alpha=-2.7$	3.20×10^{-3}	0.21
Luhman et al. (2000) **Trapezium Cluster**	[0.02–0.06] $\alpha=-0.83$	[0.06–0.08] $\alpha=+0.1$	[0.08–0.3] $\alpha=-0.8$	[0.3–2.5] $\alpha=-1.7$	[2.5–10] $\alpha=-2.7$	7.45×10^{-4}	0.22
Muench et al. (2002) **Trapezium Cluster**	[0.02–0.025] $\alpha=-6.00$	[0.025–0.12] $\alpha=-0.27$	[0.12–0.6] $\alpha=-1.15$	[0.6–10] $\alpha=-2.21$		4.61×10^{-7}	0.27

offer interesting clues concerning the reasons of IMF variations. We will consider several recent IMF determinations for the Trapezium Cluster and compare them to our IC 348 data.

Hillenbrand & Carpenter (2000) presented the results of a deep near-infrared imaging survey of a $5'\times5'$ central region of the Orion Trapezium Cluster. Their survey is sensitive to objects with masses down to 0.02 $M_\odot$ and they use their data to constrain the shape of the stellar mass function. They found that the mass function rises to a peak around 0.15 $M_\odot$ and then declines (in terms of $\mathrm{d}N/\mathrm{d}(\log M)$) across the hydrogen-burning limit. The parameterization of their mass function is given in Table 2, the resulting JLF is shown in Fig. 7. This model provides no valid description of the observed JLF for IC 348, because it predicts too many objects for $J \geq 14$ and generally produces a broader shaped JLF than observed. The KS test confirms that this model, which yields a BD fraction of 21%, is not consistent with the IMF of IC 348.

Luhman et al. (2000) presented a study of the IMF in the Trapezium cluster based on HST/NICMOS data and ground-based K-band spectra. They constructed an HR diagram to determine stellar masses and ages. The IMF they derive is listed in Table 2 and the corresponding model JLF is shown in Fig. 7. The model JLF is very similar to the Hillenbrand & Carpenter (2000) model; it has a BD fraction of 22% and also is inconsistent with the IMF of IC 348.

Muench et al. (2002) estimated the Trapezium cluster IMF from the observed K-band luminosity function. Their derived Trapezium cluster IMF (in the parameterization of their Eq. (1))

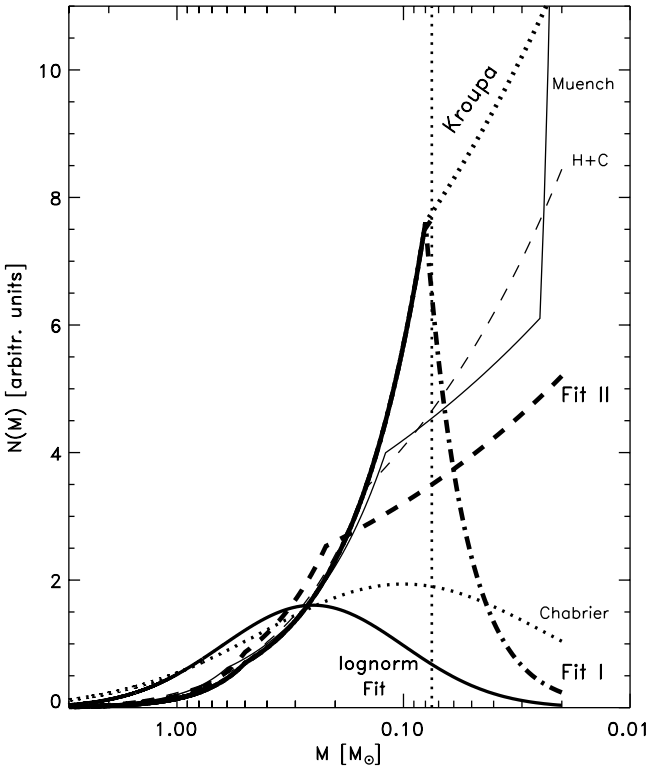

Fig. 8. Illustration of some of the IMFs used in this paper. All distributions are normalized to give the same number of objects in the 0.08−1.0 $M_\odot$ range. The thick solid line shows the Kroupa (2002) field star IMF, the sub-stellar part of which is shown by the thick dotted line. The thick dashed-dotted line shows the IMF "maximum BD fit I", the thick dashed line shows the IMF "maximum BD fit II". The solid parabolic line show the lognormal fit IMF, the dotted parabolic line represent the Chabrier (2002) field IMF. The thin solid line shows the Trapezium cluster IMF as derived by Muench et al. (2002), while the thin dashed line shows the Trapezium cluster IMF as derived by Hillenbrand & Carpenter (2000).

is listed in Table 2. Their model has a BD fraction of 27% and the model JLF is obviously inconsistent with the JLF of IC 348.

5.5. Conclusions drawn from the JLF modeling

Our modeling shows that IC 348 harbors some BDs, but the size of the sub-stellar population is relatively small. The sub-stellar part of the IMF in IC 348 is clearly different from that of the galactic field population and also the Orion Trapezium cluster. With a BD fraction of ∼10% (at most 16%) the sub-stellar population (in the 0.02−0.075 $M_\odot$ mass range) in IC 348 is about two times smaller than in the galactic field and the Trapezium cluster which have BD fractions of about 20–35%.

5.6. Comparison to the BD deficit in Taurus

It is very interesting to note that recent results suggest a similar deficit of BDs for the Taurus star forming region. Luhman (2000) investigated the IMF of the Taurus star forming region and found strong evidence for a significant deficit of BDs in that region. This result was recently confirmed and strengthened in the study by Briceno et al. (2002), who concluded that Taurus has 2× fewer brown dwarfs at 0.02−0.08 $M_\odot$ than the Orion Trapezium cluster.

Our results on IC 348 therefore provide another piece of evidence for the non-universality of the sub-stellar IMF.

6. Possible explanations for the BD deficit

How can we understand the observed differences in the sub-stellar IMF of IC 348 (and similarly Taurus) as compared to the galactic field population and the Orion Trapezium Cluster? There are a number of important differences in the physical environment of IC 348 as compared to the Trapezium Cluster. One crucial factor may be the density in the star forming environment. The stellar number density of $n_\star \sim 10^3\,\mathrm{pc}^{-3}$ in IC 348 is much lower than the density of $n_\star \sim 5\times10^4\,\mathrm{pc}^{-3}$ in the central Trapezium cluster. Briceno et al. (2002) argued that in low-density star forming environments the minimum Jeans mass may be larger, possibly explaining the BD deficit in Taurus and perhaps also in IC 348. Another important factor may lie in the different levels of supersonic turbulence in the molecular cloud, which influences the star formation process (see Mac Low & Klessen 2003 and also the discussion by Luhman 2000).

A very critical aspect we want to dicuss in some more detail is the presence or absence of massive ($M \geq 10\,M_\odot$) stars and their impact on the forming young stellar objects in their vicinity. In IC 348, the most massive star is only a B5 V star[1] with ∼6 $M_\odot$, which neither has a powerful wind nor emits strong ionizing radiation. In the Trapezium cluster, on the other hand, the strong winds and the ionizing radiation of the massive stars obviously affect nearby collapsing cloud cores and forming stars, for example by dispersing the circumstellar material of young stellar objects, as can be nicely seen in the ionized proplyds (Bally et al. 1998; see also Richling & Yorke 1998). The mass loss rates of these proplyds due to photoevaporation have been estimated to be $\approx10^{-6}\,M_\odot$/yr (Henney & O'Dell 1999), and recent numerical simulations suggest that even higher evaporation rates of up to $\approx10^{-5}\,M_\odot$/yr can be reached next to massive stars (cf. Brandner et al. 2000; Hollenbach et al. 2000). The final mass of the forming young stellar objects is therefore strongly influenced by the competition between accretion and photoevaporation. This scenario was recently explored in some detail by Whitworth & Zinnecker (2003; see also Kroupa 2001, 2002). They found that the erosion of initially more massive pre-stellar cores by the ionizing radiation from ambient massive stars can significantly diminish the accretion reservoir. In the central regions of large clusters the outer layers of the cores are eroded more rapidly than they can accrete onto a central protostar, and this can lead to the formation of BDs instead of low-mass stars. In a cluster like IC 348, i.e. in the absence

[1] We note that H98 detected a faint blue star (his number 209) in IC 348, for which the position in the color-magnitude diagram suggest that it might be a white dwarf. It is not known whether this star is a member to IC 348 or a background object; if it really is a member of the cluster, there may have been one massive star in IC 348 at one time.

of massive stars, the pre-stellar cores are unaffected by photoerosion and the protostellar objects should therefore reach systematically higher final masses; thus, a larger fraction of the forming very-low-mass objects can gain enough mass to cross the hydrogen-burning limit.

Another interesting aspect in this context is the result that the stellar part of the IMF in IC 348 is very similar to the field IMF, whereas the number of BDs is much smaller than in the field. This may be understood in the framework of the theory by Elmegreen (2000) that the IMF is the combination of two independent mass functions that combine in different ways above and below a characteristic mass. In the intermediate- to high-mass range the IMF depends primarily on the cloud structure, which seems to be rather universal and leads to very similar mass functions independent of the details of the star formation process. The turnover and the flat or declining part of the IMF is determined by the details of the transition from clumps to stars and should be sensitive to the physical conditions during the star formation process. Since the presence (or absence) of massive stars seriously affects the physical conditions during the star formation process, this would yield an interesting explanation for variations in the very-low-mass IMF.

However, it is unclear whether the impact of massive stars actually can fully explain the observed differences in the substellar populations in various environments. One problem is that photoevaporation significantly affects only the low-mass objects in the immediate vicinity of the most massive stars, whereas objects in the outer part of the cluster are not so strongly influenced (Whitworth & Zinnecker 2003). Secondly, this scenario requires that the massive stars have already entered their main-sequence phase while the low-mass objects are still in a very early evolutionary phase. This may be a particularly serious problem if the hypothesis of a very recent birth for θ^1C Ori (probably within the last few 10 000 years; see e.g. Scally & Clarke 2001) is correct.

Therefore, we finally also consider a totally different scenario. It has been suggested that BDs can form via the fragmentation of dense molecular gas in unstable multiple systems and are ejected from the dense gas before they have been able to accrete to stellar masses (Reipurth & Clarke 2001; Bate et al. 2002). In the simulations of Bate et al. (2002), this formation mechanism produced roughly the same number of BDs than stars and therefore reproduces the observed size of the BD population in the galactic field. According to this scenario, typical ejection velocities are about 3–5 km s^{-1}. In a 2 Myr period (the age of IC 348) the ejected BDs would therefore move up to about 10 pc and would be displaced up to $\sim 2^\circ$ from their formation site near the cluster center. One would therefore expect that a large fraction of the BD population has already left the cluster area and is widely dispersed.

In the Trapezium cluster, on the other hand, one would expect to see a larger BD population for two reasons: First, the cluster is younger ($\sim$1 Myr) than IC 348, therefore some of the ejected BDs have not yet moved far away. Second, due to the higher total mass of the Orion Trapezium cluster ($\sim$1100 $M_\odot$, cf. Lada & Lada 2003, versus $\sim$110 $M_\odot$ for IC 348) and its much higher central density ($n_* \sim 47\,000$ pc^{-3} for the central 0.1 pc region in the Trapezium cluster, cf. McCaughrean & Stauffer 1994, versus $n_* \sim 4200$ pc^{-3} for the central 0.1 pc region of IC 348; cf. Lada & Lada 1995) it is harder for ejected bodies to leave the much deeper gravitational potential. The mean escape velocity for IC 348 is $\sim$0.8 km s^{-1} (Herbig 1998), while the corresponding value for the Orion Trapezium cluster is $\sim$2 km s^{-1}. The statistical analysis of dynamical interactions during early cluster evolution of Sterzik & Durisen (2003) suggests that the median velocities of BDs are $\lesssim$2 km s^{-1}; this would imply that in IC 348 a large fraction of the BDs could be ejected from the cluster, while in the Orion Trapezium cluster most of the BDs would be gravitationally bound. We therefore conclude that the ejection scenario might offer a good explanation for the observed differences in the sizes of substellar populations. A direct proof for this theory, however, can only be obtained via a detailed investigation of the dynamical status of the stellar and sub-stellar cluster populations. This would require to measure the proper motions of objects with an accuracy of the order of 1 km s^{-1}. While such a project is hardly feasible with current technology, we note that it will soon be possible to obtain wide-field diffraction limited astrometric imaging with the LBT interferometer (see Zinnecker & McCaughrean 2001); in this way the validity of the ejection model could be tested.

7. Summary

Our modeling of the observed JLF in IC 348 shows that the stellar part of the IMF agrees well with the field star IMF. We find evidence that the BD population in IC 348 is about 2–3 times smaller than in the general field and is also about 2 times smaller than in the Orion Trapezium cluster. The deficit of BDs in IC 348 appears to be in line with a similar BD deficit recently found for the Taurus star forming region. These results provide evidence for the non-universality of the sub-stellar IMF and challenge current theories of very low-mass star formation and early dynamical evolution.

Final note

After completion of this work, we became aware of a recent paper by Muench et al. (2003), in which a similar near-infrared investigation of the luminosity- and mass function of IC 348 was presented. They find that the IMF of IC 348 decreases in a much steeper manner than the Trapezium IMF (as derived by Muench et al. 2002) and that the objects in the 0.025–0.08 $M_\odot$ mass range constitute only $\sim$14% of the members in IC 348, considerably less than in the Trapezium. These results agree quite well with our findings. However, in distinction to our study, they find indications for a secondary peak in the IMF of IC 348, similar to that reported by Muench et al. (2002) for the Trapezium IMF, which may increase the substellar fraction for IC 348.

Very recently, Luhman et al. (2003, [astro-ph/0304409]) presented a new census of the stellar and substellar members of IC 348. From spectroscopy of candidate cluster members they identified numerous new members, including several BDs. Their final sample of 288 spectroscopically identified cluster

members in IC 348 contains 23 BDs. The fraction of BDs in their sample, ∼8%, is in good agreement with our results.

Acknowledgements. We would like to thank the Calar-Alto staff for carrying out the observations in service mode (Observer: Ana Guijarro). We thank George H. Herbig for helpful comments and interesting discussion about IC 348. Th. P. would like to thank George H. Herbig and the other members of the Institute for Astronomy at the University of Hawaii for their kind hospitality during his visits at the Institute and for useful discussions on IC 348. This publication makes use of data products from the Two Micron All Sky Survey, which is a joint project of the University of Massachusetts and the Infrared Processing and Analysis Center/California Institute of Technology, funded by the National Aeronautics and Space Administration and the National Science Foundation.

References

Babu, G. J., & Feigelson, E. D. 1996, Astrostatistics (London: Chapman & Hall)
Bally, J., Sutherland, R. S., Devine, D., & Johnstone, D. 1998, AJ, 116, 293
Bate, M. R., Bonnell, I. A., & Bromm, V. 2002, MNRAS, 332, L65
Baraffe, I., Chabrier, G., Allard, F., & Hauschildt, P. H. 1998, A&A, 337, 403
Baraffe, I., Chabrier, G., Barman, T. S., Allard, F., & Hauschildt, P. H. 2003, A&A, 402, 701
Bizenberger, P., McCaughrean, M. J., Birk, C., Thompson, D., & Storz, C. 1998, Proc. SPIE, 3354, 825
Brandnder, W., Grebel, E. K., Chu, Y.-H., et al. 2000, AJ, 119, 292
Briceno, C., Luhmann, K. L., Hartmann, L., Stauffer, J. R., & Kirkpatrick, J. D. 2002, ApJ, 580, 317
Burrows, A., Marley, M., Hubbard, W. B., et al. 1997, ApJ, 491, 856
Cernicharo, J., Bachiller, R., & Duvert, G. 1985, A&A, 149, 273
Cernis, K. 1993, Baltic Astron., 2, 214
Chabrier, G. 2002, ApJ, 567, 304
Chabrier, G., & Baraffe, I. 2000, ARA&A, 38, 337
D'Antona, F., & Mazzitelli, I. 1997, in Cool stars in Clusters and Associations, ed. R. Pallavicini & G. Micela, Mem. S. A. It., 68, 4
de Zeeuw, P. T., Hoogerwerf, R., de Bruijne, J. H. J., Brown, A. G. A., & Blaauw, A. 1999, AJ, 117, 354
Duchene, G., Bouvier, J., & Simon, T. 1999, A&A, 343, 831
Duquennoy, A., & Mayor, M. 1991, A&A, 248, 485
Eislöffel, J., Fröbrich, D., Stanke, T., & McCaughrean, M. J. 2003, ApJ, submitted
Elmegreen, B. G. 2000, MNRAS, 311, L5
Fischer, D., & Marcy, G. 1992, ApJ, 396, 178
Harris, D. L., Morgan, W. W., & Roman, N. G. 1954, ApJ, 119, 622
Henney, W. J., & O'Dell, C. R. 1999, AJ, 118, 2350
Herbig, G. H. 1954, PASP, 66, 19
Herbig, G. H. 1998, ApJ, 497, 736 [H98]
Hillenbrand, L. A., & Carpenter, J. M. 2000, ApJ, 540, 236
Hollenbach, D. J., Yorke, H. W., Johnstone, D. 2000, in Protostars and Planets IV, ed. V. Mannings, A. P. Boss, & S. S. Russell (Tucson: University of Arizona Press), 401
Kenyon, S. J., & Hartmann, L. 1995, ApJS, 101, 117
Kroupa, P. 2001, MNRAS, 322, 231
Kroupa, P. 2002, Science, 295, 82
Lada, E. A., & Lada, C. J. 1995, AJ, 109, 1682
Lada, E. A., & Lada, C. J. 2003, ARA&A, in press
Lada, E. A., Lada, C. J., & Muench, A. 1998, in The Stellar Initial Mass Function, ed. G. Gilmore, D. Howell, ASP Conf. Ser., 142, 107
Leggett, S. K., Allard, F., Berriman, G., Dahn, C. C., Hauschildt, P. H. 1996, ApJS, 104, 117
Liu, M. C. 2002, in The twelfth Cambridge Workshop on Cool Stars, Stellar Systems and the Sun, ASP Conf. Ser., in press
Luhman, K. L., Rieke, G. H., Lada, C. J., & Lada, E. A. 1998, ApJ, 508, 347 (L98)
Luhman, K. L. 1999, ApJ, 525, 466
Luhman, K. L. 2000, ApJ, 544, 1044
Luhman, K. L., Rieke, G. H., Young, E. T., et al. 2000, ApJ, 540, 1016
Mac Low, M.-M., & Klessen, R. S. 2003, Rev. Mod. Phys, in press
Martin, E., et al. 2003, in IAU Symp. 211: Brown Dwarfs, ASP Conf. Ser., in press
McCaughrean, M. J., & Stauffer, J. R. 1994, AJ, 108,1382
McCaughrean, M. J., Rayner, J. T., & Zinnecker, H. 1994, ApJ, 436, L189
McCaughrean, M. J., Zinnecker, H., Rayner, J. T., & Stauffer, J. 1995, in The bottom of the main sequence – and beyond, ed. C. G. Tinney, ESO Astrophys. Symp. (Springer Verlag), 209
Miller G. E., & Scalo J. M. 1979, ApJS, 41, 513
Muench, A. A., Lada, E. A., Lada, C. J., & Alves, J. 2002, ApJ, 573, 366
Muench, A. A., Lada, E. A., Lada, C. J., et al. 2003, AJ, 125,2029
Najita, J. R., Tiede, G. P., & Carr, J. S. 2000, ApJ, 541, 977 [N00]
Oppenheimer, B. R., Kulkarni, S. R., Matthews, K., Nakajima, T. 1995, Science, 270, 1478
Oppenheimer, B. R., Kulkarni, S. R., & Stauffer, J. R. 2000, in Protostars and Planets IV, ed. V. Mannings, A. P. Boss, S. S. Russell (Tucson: University of Arizona Press), 1313
Palla, F., & Stahler S. W. 1999, ApJ, 525,772
Preibisch, Th., & Zinnecker, H. 1999, AJ, 117, 2381
Preibisch, Th., & Zinnecker, H. 2001, AJ, 122, 866
Preibisch, Th., & Zinnecker, H. 2002, AJ, 123, 1613
Preibisch, Th., Brown, A., Bridges, T., Guenther, E., & Zinnecker, H. 2002, AJ, 124, 404
Preibisch, Th., Zinnecker, H., & Herbig, G. H. 1996, A&A, 310, 456
Rebolo, R., Zapatero Osori, M. R., & Martin, E. L. 1995, Nature, 227, 129
Reid, I. N., Kirkpatrick, J. D., Liebert, J., et al. 1999, ApJ, 521, 613
Reipurth, B., & Clarke, C. 2001, AJ, 122, 432
Richling, S., & Yorke, H. W. 1998, A&A, 340, 408
Rieke, G. H., & Lebofsky, M. J. 1985, ApJ, 288, 618
Ripepi, V., Palla, F., Marconi, M., et al. 2002, A&A, 391, 587
Scally, A., & Clarke, C. 2001, MNRAS, 325, 449
Scalo, J. 1998, in The Stellar Initial Mass Function, ed. G. Gilmore, D. Howell, ASP Conf. Ser., 142, 201
Schlegel, D. J., Finkenbeiner, D. P., & Davis, M. 1998, ApJ, 500, 525
Sterzik, M. F., & Durisen, R. H. 2003, A&A, 400, 1031
White, R. J., Ghez, A. M., Reid, I. N., & Schultz, G. 1999, ApJ, 520, 811
Whitworth, A., & Zinnecker, H. 2003, A&A, submitted
Yorke, H. W. 1986, ARA&A, 24, 49
Zinnecker, H., & McCaughrean, M. J. 2001, in Science with the Large Binocular Telescope, ed. T. Herbst, p. 137
Zinnecker, H., McCaughrean, M. J., & Wilking, B. A. 1993, in Protostars and Planets III, ed. E. H. Levy, & J. I. Lumine (University of Arizona Press), 429

Online Material

Table 1. *J*-band magnitudes of the sources detected in our IC 348 image. The source names contain the J2000 coorinates.

IC348-J	*J* [mag]	IC348-J	*J* [mag]	IC348-J	*J* [mag]
034350.6+321059	18.69	034352.4+321049	19.93	034354.6+320853	19.73
034350.6+321231	19.46	034352.5+321121	20.87	034354.6+320723	17.47
034350.7+321306	14.20	034352.5+320705	19.57	034354.7+320912	19.64
034350.7+321125	19.98	034352.6+320118	19.62	034354.7+321320	20.31
034350.8+321433	19.65	034352.7+320736	18.83	034354.7+320856	18.26
034350.9+321133	20.45	034352.7+320752	20.13	034354.7+321210	17.02
034350.9+321429	20.65	034352.7+321320	20.15	034354.8+321129	17.50
034351.0+321513	16.30	034352.7+321326	19.07	034354.8+321340	17.27
034351.0+321127	19.17	034352.7+320652	18.40	034354.9+320929	20.16
034351.1+321139	17.84	034352.7+321204	18.15	034354.9+321427	19.53
034351.1+320701	16.94	034352.8+321441	18.09	034355.0+321211	19.18
034351.1+321359	20.01	034352.8+320814	18.42	034355.1+321426	18.51
034351.1+321348	18.74	034352.8+321350	19.67	034355.1+320714	14.10
034351.2+321525	20.02	034352.8+321523	19.47	034355.1+321326	15.89
034351.2+320928	18.73	034352.8+320617	19.97	034355.1+321612	19.72
034351.2+321045	17.76	034352.8+320901	18.89	034355.2+321006	16.37
034351.2+321430	20.35	034353.1+321306	17.40	034355.3+320154	19.90
034351.3+320656	17.13	034353.1+320954	19.55	034355.3+320753	13.57
034351.3+321309	10.25	034353.2+320844	14.57	034355.3+321402	19.60
034351.3+320720	19.28	034353.2+321555	18.14	034355.3+321700	17.88
034351.3+321154	17.32	034353.3+321202	15.58	034355.4+321102	20.25
034351.3+320812	19.69	034353.3+320924	19.32	034355.4+321655	19.74
034351.4+320504	17.80	034353.3+321300	14.07	034355.4+321249	19.70
034351.4+321141	19.66	034353.4+320925	17.91	034355.5+320704	17.98
034351.4+321508	20.63	034353.5+320726	16.20	034355.5+321001	19.22
034351.4+320708	19.16	034353.5+321040	19.77	034355.5+320931	11.28
034351.4+321518	17.81	034353.5+321312	17.47	034355.6+320956	20.03
034351.5+321630	20.41	034353.5+321418	15.78	034355.6+321451	18.54
034351.5+321028	20.02	034353.6+321017	16.48	034355.6+321343	20.20
034351.6+320740	19.87	034353.6+321715	20.09	034355.6+321530	16.32
034351.6+320844	18.74	034353.6+321229	20.02	034355.6+321325	16.81
034351.6+321124	16.72	034353.7+320905	17.99	034355.7+321701	18.75
034351.6+321240	20.01	034353.7+321145	19.49	034355.7+320912	19.83
034351.6+321313	19.33	034353.7+320805	20.10	034355.7+321504	20.14
034351.6+320552	18.14	034353.8+321334	19.14	034355.9+321603	19.68
034351.6+321556	12.99	034353.8+321217	17.57	034355.9+320921	19.18
034351.7+321347	18.70	034353.8+320730	13.68	034356.0+320212	12.34
034351.7+320526	19.91	034353.9+321054	16.70	034356.0+320928	19.83
034351.8+320632	19.09	034353.9+320225	19.75	034356.0+320943	20.09
034351.9+320220	20.20	034353.9+321311	19.82	034356.1+320306	19.66
034351.9+320211	20.04	034353.9+321255	20.11	034356.1+320734	19.91
034351.9+321206	20.71	034354.0+321339	18.29	034356.1+321443	19.79
034351.9+321627	19.99	034354.0+320842	18.60	034356.2+321403	17.85
034352.0+321524	19.72	034354.1+320933	18.88	034356.2+321605	18.07
034352.0+321201	16.96	034354.2+320212	18.04	034356.2+321255	19.11
034352.0+320339	13.79	034354.2+321705	20.18	034356.2+320836	12.58
034352.0+320948	18.04	034354.2+320611	19.59	034356.4+320959	15.38
034352.0+321326	19.45	034354.2+321147	16.71	034356.4+321633	19.89
034352.0+320949	19.34	034354.3+321333	20.35	034356.5+321516	19.77
034352.1+321413	18.94	034354.3+320148	20.22	034356.5+321506	18.20
034352.2+321350	20.14	034354.4+320242	20.02	034356.6+321325	19.87
034352.3+320732	18.60	034354.5+321327	19.28	034356.6+321114	19.55
034352.3+321534	19.31	034354.5+320210	19.93	034356.6+321720	19.99
034352.3+321527	20.67	034354.5+321014	13.25	034356.7+321516	16.95
034352.3+321214	20.17	034354.6+321249	17.30	034356.7+321039	19.25
034352.4+321432	21.19	034354.6+320754	19.56	034356.7+320721	19.46
034352.4+321029	20.11	034354.6+320853	19.73	034356.7+321510	19.17

Table 1. continued.

IC348-J	*J* [mag]	IC348-J	*J* [mag]	IC348-J	*J* [mag]
034356.9+321316	19.40	034359.5+321555	12.84	034402.3+320923	18.04
034356.9+321415	17.66	034359.6+320604	17.63	034402.4+321015	14.95
034356.9+321522	20.20	034359.6+321143	19.05	034402.4+321305	18.92
034356.9+320534	19.86	034359.6+320154	13.84	034402.4+321102	18.79
034356.9+321428	16.79	034359.7+321549	18.84	034402.4+321127	16.89
034357.0+321400	19.92	034359.7+321455	19.49	034402.4+321141	17.20
034357.0+321434	19.87	034359.7+321403	12.25	034402.4+321720	16.24
034357.2+320133	15.72	034359.7+321559	16.28	034402.5+321154	18.02
034357.3+321258	12.75	034359.8+320921	19.22	034402.5+321547	18.37
034357.3+320805	20.01	034359.9+320441	14.26	034402.5+321523	19.50
034357.4+321632	19.85	034359.9+321047	13.88	034402.6+320134	12.94
034357.5+321454	19.80	034359.9+321115	12.21	034402.6+320547	20.26
034357.5+321711	19.31	034359.9+320908	17.87	034402.6+321415	17.54
034357.5+321551	19.46	034360.0+320740	18.90	034402.7+321304	19.07
034357.6+321508	19.34	034400.0+321328	19.31	034402.7+320954	19.90
034357.6+320137	14.60	034400.1+320654	18.29	034402.9+321528	19.78
034357.6+321449	14.87	034400.2+321548	19.50	034402.9+320815	19.34
034357.6+321320	17.46	034400.2+320655	19.85	034402.9+321228	17.00
034357.7+320914	18.12	034400.2+321458	19.54	034402.9+320615	16.95
034357.8+320750	17.68	034400.2+321354	17.17	034403.0+320636	19.67
034357.8+321158	18.59	034400.3+321132	19.36	034403.0+321720	16.83
034357.8+321619	17.33	034400.5+320432	19.57	034403.0+321619	19.80
034357.9+321544	20.12	034400.5+320742	19.00	034403.2+320948	18.61
034357.9+321234	17.73	034400.5+321058	17.80	034403.4+320658	17.82
034358.0+321048	19.92	034400.6+321521	17.15	034403.5+321523	17.48
034358.0+321144	16.33	034400.6+321344	19.58	034403.5+321606	20.18
034358.0+320633	19.84	034400.6+321207	19.69	034403.5+321143	15.32
034358.1+320946	9.85	034400.7+320419	19.42	034403.6+320232	14.48
034358.1+321556	17.57	034400.8+321107	18.43	034403.6+320235	14.40
034358.2+321357	14.10	034400.9+321240	20.02	034403.6+320518	17.55
034358.2+321432	14.10	034400.9+320818	20.24	034403.6+321639	14.67
034358.2+320946	12.00	034400.9+321442	19.89	034403.6+320520	15.50
034358.2+321015	18.42	034400.9+320538	18.76	034403.6+321007	18.05
034358.2+321239	17.70	034400.9+321056	19.17	034403.7+320548	20.20
034358.5+320835	18.77	034401.0+321350	20.27	034403.7+320819	18.38
034358.6+320959	17.74	034401.1+321532	17.33	034403.7+321015	18.07
034358.7+321509	19.83	034401.1+321648	19.08	034403.8+320648	18.67
034358.7+321517	19.46	034401.2+321058	19.75	034403.9+321042	18.69
034358.8+320830	18.92	034401.2+321230	19.39	034403.9+321613	19.34
034358.8+321225	16.00	034401.3+321341	19.05	034403.9+321637	19.29
034358.9+321053	19.75	034401.4+320549	16.48	034404.0+321327	19.68
034358.9+321127	12.15	034401.4+321022	19.26	034404.1+320717	13.03
034358.9+321023	17.68	034401.5+321553	17.78	034404.2+320949	19.13
034359.0+320958	15.74	034401.5+321450	18.84	034404.2+321050	19.52
034359.0+321715	19.98	034401.5+321541	20.46	034404.2+320801	18.38
034359.1+321421	13.19	034401.8+321632	19.10	034404.2+321406	17.52
034359.1+320829	19.48	034401.9+321253	17.79	034404.2+320750	19.85
034359.2+320556	14.76	034401.9+321121	15.18	034404.2+320938	13.65
034359.2+320933	19.44	034402.0+321426	19.56	034404.2+321349	12.52
034359.2+321430	20.27	034402.0+321536	20.03	034404.3+321550	14.92
034359.2+321450	18.79	034402.0+321001	18.82	034404.3+321233	19.48
034359.2+320250	18.33	034402.1+321621	19.09	034404.4+321555	19.96
034359.2+321402	18.89	034402.1+320615	19.96	034404.4+321100	19.92
034359.3+321705	20.14	034402.2+320731	20.30	034404.4+321545	20.21
034359.3+320625	17.62	034402.3+321430	18.38	034404.4+320453	14.25
034359.5+321505	19.34	034402.3+321128	18.86	034404.5+321015	20.36

Table 1. continued.

IC348-J	*J* [mag]	IC348-J	*J* [mag]	IC348-J	*J* [mag]
034404.5+321709	20.52	034407.2+321337	19.67	034410.6+321055	17.93
034404.5+321113	19.61	034407.3+321433	17.76	034410.6+321144	14.98
034404.6+320838	20.34	034407.3+320948	19.57	034410.6+321431	17.95
034404.6+321421	18.98	034407.4+321021	18.65	034410.7+321406	19.25
034404.9+320634	18.50	034407.4+321550	19.67	034410.8+320830	18.93
034404.9+320650	19.45	034407.4+321655	20.96	034410.8+321215	19.23
034404.9+320723	19.28	034407.5+320408	13.47	034410.8+321300	16.39
034404.9+321044	18.86	034407.5+321049	18.92	034410.9+320441	17.62
034404.9+321656	17.51	034407.6+321330	19.95	034411.0+320315	19.85
034404.9+320716	19.22	034407.7+320505	14.12	034411.0+320143	16.95
034405.0+320953	11.52	034407.8+320238	20.18	034411.1+320534	19.58
034405.0+321538	18.62	034407.8+321409	19.64	034411.2+320816	12.83
034405.2+320908	20.39	034407.8+321538	19.28	034411.3+320611	12.39
034405.2+321228	19.38	034407.8+320350	19.39	034411.3+321416	19.66
034405.2+321406	19.20	034407.8+320635	19.66	034411.3+320906	19.66
034405.2+320259	19.32	034407.8+321440	16.88	034411.4+320850	18.70
034405.3+320802	14.23	034407.8+321609	20.93	034411.5+321212	17.71
034405.3+321311	16.59	034407.9+320754	19.93	034411.6+321424	20.05
034405.4+320807	18.94	034407.9+321058	19.29	034411.6+320312	12.81
034405.4+321357	19.57	034408.0+321404	17.93	034411.6+320427	19.07
034405.5+320900	20.42	034408.0+321244	19.38	034411.7+321217	19.43
034405.5+321344	17.33	034408.1+320656	13.59	034412.1+320624	19.06
034405.7+321044	16.06	034408.3+321056	19.10	034412.2+321252	18.14
034405.8+321229	12.29	034408.3+321445	18.72	034412.2+321134	19.62
034405.8+321552	19.11	034408.3+321538	15.81	034412.2+321247	19.66
034405.9+320903	17.73	034408.3+321357	17.69	034412.3+321102	19.82
034405.9+320639	19.27	034408.4+320927	19.79	034412.3+321221	17.91
034405.9+321212	18.08	034408.5+320715	8.77	034412.4+321407	17.81
034405.9+320900	19.06	034408.5+320959	19.24	034412.5+320332	20.49
034405.9+320420	19.83	034408.5+321613	19.89	034412.8+321055	14.71
034406.0+321532	14.24	034408.6+321631	19.44	034412.8+321330	20.49
034406.0+320952	18.47	034408.7+320803	18.17	034412.8+321232	17.74
034406.0+321059	19.25	034408.8+321521	19.13	034412.9+321324	18.28
034406.1+321454	18.28	034408.8+320633	19.66	034413.0+320135	15.85
034406.1+320926	18.14	034408.9+321044	19.17	034413.0+321315	14.37
034406.1+320707	13.70	034408.9+321610	11.37	034413.0+320435	19.88
034406.1+321506	16.64	034408.9+320929	20.05	034413.2+320747	19.08
034406.3+321119	19.52	034409.0+321257	19.32	034413.3+320931	19.97
034406.3+321035	19.76	034409.0+321329	18.30	034413.3+320444	19.07
034406.4+321410	18.81	034409.1+321529	18.88	034413.5+320300	15.36
034406.4+321700	19.94	034409.2+320613	20.21	034413.6+321439	15.30
034406.5+321441	20.23	034409.2+320708	8.82	034413.7+321408	19.70
034406.5+321202	16.53	034409.2+321157	20.08	034413.7+320736	19.31
034406.5+321101	20.08	034409.2+320237	15.68	034413.9+321409	19.01
034406.6+321640	19.50	034409.4+321110	18.55	034413.9+321027	18.75
034406.6+321720	16.67	034409.4+321419	16.67	034413.9+320438	19.35
034406.6+320651	19.42	034409.5+320415	20.28	034414.0+320539	18.14
034406.6+320741	20.36	034409.7+320738	19.48	034414.1+320354	18.71
034406.7+320922	20.11	034409.8+321307	17.81	034414.1+321028	12.52
034406.8+320754	13.03	034409.9+320302	18.05	034414.2+321204	16.34
034406.8+320440	13.76	034410.0+321123	19.70	034414.2+321403	19.57
034406.9+321228	20.11	034410.0+320941	14.24	034414.4+321411	20.17
034406.9+320155	18.31	034410.0+321502	20.13	034414.5+321400	17.93
034407.0+320826	19.40	034410.0+320804	19.35	034414.5+320403	18.90
034407.0+321101	18.20	034410.1+320404	13.34	034414.7+321225	19.56
034407.0+321629	20.58	034410.2+320734	14.70	034414.9+321405	17.78
034407.1+320844	17.14	034410.3+321400	16.65	034414.9+320612	18.07
034407.2+321600	21.16	034410.6+321152	18.83	034414.9+321344	18.07

Table 1. continued.

IC348-J	*J* [mag]	IC348-J	*J* [mag]	IC348-J	*J* [mag]
034414.9+320945	18.39	034418.2+320456	12.08	034421.2+320114	16.52
034415.0+321053	17.62	034418.2+321140	15.11	034421.3+320502	12.98
034415.0+321120	19.26	034418.2+321133	19.98	034421.3+321237	13.81
034415.1+320352	18.77	034418.2+321422	15.98	034421.3+321156	12.68
034415.1+320343	20.10	034418.2+320959	13.22	034421.4+321121	17.74
034415.1+320427	19.08	034418.3+320732	13.78	034421.5+320305	19.70
034415.1+320504	20.49	034418.3+321112	19.37	034421.6+320253	19.31
034415.2+320715	20.16	034418.4+320327	19.16	034421.6+321017	12.53
034415.4+320603	19.76	034418.5+320642	19.99	034421.6+321445	18.05
034415.5+320234	12.98	034418.6+321253	14.03	034421.6+320141	20.28
034415.5+320953	18.56	034418.7+321132	18.13	034421.6+320508	20.25
034415.6+321014	16.42	034418.8+320832	17.58	034421.6+321037	12.47
034415.6+321108	19.16	034418.9+321133	16.27	034421.6+321347	15.83
034415.6+320921	14.60	034419.0+320736	14.59	034421.7+320624	12.57
034415.6+321445	19.82	034419.1+321411	19.71	034421.7+321136	19.21
034415.8+321431	14.95	034419.2+320930	11.65	034421.7+321114	17.08
034415.9+321150	17.01	034419.2+321333	19.25	034421.8+321231	13.10
034416.0+321209	16.35	034419.2+320600	14.46	034421.8+321413	19.91
034416.1+320533	17.79	034419.2+320848	19.94	034421.9+321200	18.63
034416.1+321100	18.83	034419.2+320634	19.01	034421.9+321211	12.28
034416.2+321118	19.58	034419.2+321018	18.54	034422.0+321400	17.47
034416.2+320540	17.76	034419.2+320734	12.79	034422.0+321429	18.96
034416.2+321218	16.87	034419.2+321216	19.18	034422.1+321327	19.57
034416.2+321345	19.51	034419.3+320623	19.96	034422.1+321410	18.73
034416.3+321209	18.73	034419.3+321248	18.88	034422.1+320653	19.83
034416.3+320135	19.81	034419.4+321449	19.93	034422.2+320333	18.45
034416.3+321157	18.80	034419.4+321410	16.34	034422.3+320543	12.55
034416.3+321254	17.06	034419.4+321430	20.31	034422.3+321201	12.52
034416.3+321313	19.35	034419.5+321428	19.49	034422.4+321301	18.65
034416.4+320955	11.32	034419.5+320605	18.60	034422.4+321048	20.01
034416.5+321029	17.98	034419.6+320224	14.94	034422.5+320746	20.41
034416.5+320533	13.39	034419.6+320557	18.75	034422.6+320127	15.30
034416.6+320525	18.67	034419.6+320731	20.51	034422.6+320154	12.11
034416.8+321350	18.42	034419.7+320645	16.93	034422.7+320142	15.27
034417.0+321013	17.45	034419.7+320848	19.99	034422.8+320205	17.72
034417.1+321317	20.42	034419.7+320632	20.23	034423.0+320718	18.29
034417.1+320153	18.23	034419.8+320324	19.22	034423.0+321440	14.17
034417.1+321115	19.32	034419.8+321308	18.82	034423.0+321157	12.57
034417.2+320520	19.61	034419.8+320852	20.66	034423.1+321426	18.94
034417.2+320534	20.27	034420.0+320848	19.76	034423.2+320722	20.62
034417.2+321349	18.40	034420.0+320645	13.57	034423.3+320717	20.62
034417.3+321107	19.30	034420.2+320856	12.67	034423.3+320154	15.00
034417.4+321239	20.07	034420.3+320544	14.32	034423.4+320229	17.81
034417.4+320835	16.74	034420.3+320657	20.18	034423.5+320814	18.72
034417.6+320529	17.45	034420.3+320522	20.50	034423.6+320934	13.42
034417.6+321244	20.31	034420.4+320320	17.87	034423.6+320711	14.48
034417.7+321122	18.04	034420.6+320751	19.01	034423.6+320153	14.64
034417.7+320136	20.22	034420.6+320312	16.70	034423.7+320646	12.24
034417.8+320447	13.33	034420.7+321015	20.39	034423.7+321241	20.23
034417.8+321121	18.04	034420.9+321004	18.47	034423.8+321156	14.85
034417.8+321040	20.83	034420.9+321237	13.94	034423.8+321112	20.48
034417.9+321220	12.18	034420.9+320858	19.74	034423.8+321008	19.46
034417.9+321408	19.71	034421.0+320424	18.78	034423.9+321421	19.26
034417.9+321435	19.70	034421.0+320800	18.70	034424.0+320908	20.31
034418.0+320157	18.32	034421.0+321335	17.84	034424.0+320533	18.97
034418.1+321053	15.50	034421.1+320738	11.72	034424.0+321059	10.75
034418.1+320833	17.15	034421.2+320616	15.28	034424.1+321314	17.69

Table 1. continued.

IC348-J	*J* [mag]	IC348-J	*J* [mag]	IC348-J	*J* [mag]
034424.3+320611	17.48	034427.3+320717	14.35	034429.9+320403	19.37
034424.3+321019	11.40	034427.3+321421	12.77	034430.0+320422	20.23
034424.3+320758	15.59	034427.3+320755	18.45	034430.0+320921	13.36
034424.4+320614	20.50	034427.4+321401	16.11	034430.0+320939	15.03
034424.4+320144	15.74	034427.5+320616	18.99	034430.0+320755	19.37
034424.5+321305	19.14	034427.5+320218	18.37	034430.0+320849	14.53
034424.6+320357	12.91	034427.5+320624	20.05	034430.0+321623	20.01
034424.6+321002	14.05	034427.5+320658	20.47	034430.1+320541	18.14
034424.6+321140	17.59	034427.5+320225	20.14	034430.1+320118	15.09
034424.6+321132	19.16	034427.6+320302	15.23	034430.3+320742	13.90
034424.7+321015	9.37	034427.6+320447	19.10	034430.3+321135	16.57
034424.8+320543	19.85	034427.6+320843	17.84	034430.3+320944	16.25
034424.9+321348	17.05	034427.6+320944	18.93	034430.4+320205	20.22
034424.9+320540	19.87	034427.7+321355	14.82	034430.4+320607	19.31
034425.0+320446	18.23	034427.7+320851	20.07	034430.4+321310	18.73
034425.2+320632	20.40	034427.8+320800	17.54	034430.4+321457	15.98
034425.2+320449	20.25	034427.9+321052	13.82	034430.5+321230	16.96
034425.2+320536	17.21	034427.9+320731	12.14	034430.6+320629	12.81
034425.3+321012	12.68	034428.0+320519	14.88	034430.7+320933	19.97
034425.3+320831	20.16	034428.0+320840	18.75	034430.8+320955	9.84
034425.4+321316	20.31	034428.2+321029	20.50	034430.9+321251	20.24
034425.4+320438	19.23	034428.2+321305	17.93	034430.9+321125	17.59
034425.4+321356	16.86	034428.2+321354	19.34	034431.0+320244	15.63
034425.4+321405	16.83	034428.2+321219	16.83	034431.0+320558	21.11
034425.5+320612	20.68	034428.4+321122	14.36	034431.0+320546	14.03
034425.5+320745	19.37	034428.4+321110	19.69	034431.0+320946	18.93
034425.5+320617	12.90	034428.5+320722	11.66	034431.1+320146	17.40
034425.6+320625	15.23	034428.5+321200	18.93	034431.2+320558	15.12
034425.6+321229	11.85	034428.6+320424	19.24	034431.2+320849	16.53
034425.6+321130	12.51	034428.6+320441	20.02	034431.2+321327	19.59
034425.6+321429	18.66	034428.7+320527	20.23	034431.2+320621	8.31
034425.8+320905	14.56	034428.7+320150	17.95	034431.2+321447	15.24
034425.8+321058	17.20	034428.7+320207	18.61	034431.3+320928	14.05
034425.8+320453	20.84	034428.7+320940	19.89	034431.3+320730	16.99
034425.9+321338	19.92	034428.8+321343	17.16	034431.3+320811	17.34
034425.9+321106	16.06	034428.8+320423	15.08	034431.4+321047	13.38
034425.9+320805	19.27	034428.8+321032	19.13	034431.4+320302	19.84
034426.0+320313	19.21	034428.9+320158	19.91	034431.4+321129	13.52
034426.0+320430	10.09	034428.9+320702	19.66	034431.5+320706	17.55
034426.1+320238	19.74	034428.9+320259	20.15	034431.6+320844	10.66
034426.4+320809	17.87	034428.9+320231	16.17	034431.6+320945	17.69
034426.4+320827	19.93	034428.9+320138	15.53	034431.6+321454	19.88
034426.5+321352	18.78	034429.0+321402	17.07	034431.6+321548	19.50
034426.5+320820	15.43	034429.1+320255	19.49	034431.7+320513	19.62
034426.6+320358	11.80	034429.1+320751	14.02	034431.7+320653	13.52
034426.7+320236	14.62	034429.1+320757	13.59	034431.7+320432	19.86
034426.7+320834	19.68	034429.1+321448	19.11	034431.8+321244	14.65
034426.7+320820	12.89	034429.2+320115	14.54	034431.8+321400	16.58
034426.7+320930	20.05	034429.3+321026	18.23	034431.9+321515	19.90
034426.8+320649	20.13	034429.4+320259	20.22	034431.9+321546	14.19
034426.8+321218	18.19	034429.5+320404	14.31	034432.0+321144	10.15
034426.9+320926	16.54	034429.6+320137	18.55	034432.2+320511	19.37
034426.9+321250	16.33	034429.6+320102	20.36	034432.3+320135	16.25
034427.0+320443	11.95	034429.6+320729	20.42	034432.3+320729	20.21
034427.1+320304	20.43	034429.7+321552	18.53	034432.4+320327	14.99
034427.2+320346	17.29	034429.7+320552	13.61	034432.4+320803	16.07
034427.2+321006	18.42	034429.7+321039	11.95	034432.6+320842	11.24
034427.2+321037	13.57	034429.8+320515	19.60	034432.6+320856	12.10

Table 1. continued.

IC348-J	*J* [mag]	IC348-J	*J* [mag]	IC348-J	*J* [mag]
034432.7+320415	13.76	034435.0+320736	10.97	034437.5+321611	19.49
034432.8+320837	10.28	034435.2+321105	19.82	034437.5+321156	16.77
034432.8+320915	12.33	034435.3+320332	18.32	034437.6+320344	19.59
034432.8+320413	13.76	034435.4+320736	12.09	034437.6+321113	19.98
034432.9+321450	20.15	034435.4+321004	7.92	034437.6+320832	18.89
034432.9+321518	19.99	034435.4+321104	19.92	034437.8+321217	12.87
034433.1+321459	14.50	034435.4+320856	13.20	034437.8+320315	19.92
034433.1+320355	20.18	034435.5+320804	13.56	034437.8+321007	13.95
034433.2+321528	12.50	034435.5+320212	19.19	034437.9+320508	18.01
034433.2+320858	19.86	034435.6+320518	19.01	034437.9+320522	17.51
034433.2+321257	15.17	034435.6+320223	18.78	034437.9+320804	11.66
034433.3+320752	17.25	034435.7+320248	17.79	034437.9+321500	19.44
034433.3+320939	12.39	034435.7+320303	14.21	034438.0+320329	11.42
034433.4+321031	16.58	034435.7+320453	13.79	034438.0+321137	13.22
034433.5+320316	19.89	034435.8+321101	19.04	034438.1+320433	15.85
034433.5+321118	19.31	034435.9+321502	13.20	034438.1+321645	15.29
034433.7+321336	17.51	034435.9+321504	13.79	034438.1+321021	14.27
034433.7+320521	18.15	034435.9+321553	12.95	034438.1+321031	19.02
034433.7+320547	17.41	034435.9+321527	19.55	034438.2+321646	16.38
034433.7+320416	20.05	034435.9+321117	15.72	034438.3+321647	19.26
034433.8+321321	20.14	034436.0+320924	13.83	034438.3+321047	18.64
034433.8+321555	19.34	034436.1+320320	19.95	034438.4+321300	12.77
034433.9+320340	19.91	034436.1+321715	18.85	034438.4+320845	19.51
034433.9+320730	17.12	034436.1+320717	19.28	034438.5+320735	11.17
034434.0+321403	17.38	034436.2+321623	17.56	034438.5+320652	18.66
034434.0+320854	11.83	034436.2+320706	18.60	034438.5+321220	20.04
034434.0+321541	18.94	034436.3+321304	17.12	034438.5+320800	11.93
034434.1+320657	14.02	034436.3+320714	20.30	034438.6+321104	18.22
034434.1+321103	19.36	034436.3+321419	17.23	034438.6+321524	16.72
034434.2+321635	14.06	034436.3+320513	19.96	034438.6+320506	12.46
034434.2+320946	6.76	034436.4+320305	16.69	034438.6+321528	19.59
034434.3+321240	15.35	034436.4+320754	19.99	034438.6+320748	20.05
034434.3+321448	18.67	034436.4+320919	14.30	034438.7+320856	12.41
034434.3+321049	12.13	034436.4+321029	16.21	034438.7+320841	11.17
034434.3+321606	14.34	034436.5+320317	18.56	034438.8+320306	17.73
034434.4+320422	14.14	034436.6+320903	19.71	034438.8+321447	16.18
034434.4+321416	18.80	034436.6+320344	16.70	034438.9+320636	13.98
034434.4+320754	18.35	034436.7+320725	19.15	034438.9+321502	19.86
034434.5+320625	13.34	034436.7+320901	20.57	034438.9+320608	17.05
034434.5+320843	16.04	034436.7+321248	19.96	034439.0+320319	14.27
034434.5+321333	18.44	034436.8+321328	20.42	034439.0+321320	19.96
034434.6+320213	19.43	034436.9+321418	18.99	034439.0+320514	18.99
034434.6+320329	19.93	034436.9+321436	15.56	034439.2+320813	14.84
034434.6+321017	15.89	034437.0+320609	18.71	034439.2+320918	10.05
034434.7+320339	19.78	034437.0+320645	9.19	034439.2+320945	12.35
034434.7+321554	13.15	034437.0+320834	12.95	034439.2+320735	10.84
034434.7+321600	14.98	034437.0+320947	20.18	034439.3+321443	18.06
034434.7+321516	19.27	034437.0+321656	18.65	034439.3+320928	16.23
034434.8+320519	19.98	034437.1+320610	19.25	034439.4+321008	13.74
034434.8+321550	19.62	034437.2+320748	18.14	034439.6+320527	20.41
034434.8+321117	12.72	034437.2+320915	12.50	034439.8+321345	18.74
034434.9+320953	12.55	034437.3+321609	20.08	034439.8+321558	13.34
034434.9+320633	11.50	034437.3+320711	13.90	034439.9+321247	20.16
034434.9+320604	20.06	034437.3+321255	17.93	034439.9+320613	15.79
034434.9+321500	16.94	034437.4+320317	20.22	034440.0+320649	20.09
034434.9+321627	20.24	034437.4+321224	13.08	034440.1+321134	11.66
034435.0+321530	13.13	034437.4+320611	12.06	034440.1+321427	12.50
034435.0+320857	14.77	034437.4+320900	12.46	034440.2+320912	13.22

Table 1. continued.

IC348-J	*J* [mag]	IC348-J	*J* [mag]	IC348-J	*J* [mag]
034440.2+321414	16.70	034442.6+321341	18.72	034444.9+320937	18.28
034440.2+321506	18.38	034442.6+320302	20.36	034444.9+321411	15.81
034440.2+320932	13.86	034442.6+320619	12.54	034445.0+321336	12.59
034440.2+321040	19.76	034442.6+321117	19.74	034445.0+320319	19.33
034440.3+320714	18.91	034442.6+320251	20.36	034445.0+320811	18.23
034440.3+321426	17.09	034442.6+320700	19.56	034445.1+321413	13.47
034440.4+320258	20.07	034442.6+321541	15.01	034445.1+320933	19.18
034440.4+321527	20.22	034442.7+320833	13.12	034445.1+321124	19.67
034440.5+320304	17.74	034442.9+320535	19.73	034445.1+321356	18.88
034440.7+320941	15.18	034442.9+321029	17.98	034445.2+320817	18.26
034440.8+320213	20.14	034442.9+320306	19.59	034445.2+320119	16.21
034440.8+321306	13.55	034442.9+321318	19.04	034445.2+321055	14.52
034440.8+320239	19.63	034443.0+320654	14.76	034445.2+320224	18.01
034440.8+320320	18.68	034443.0+321015	13.38	034445.2+320341	18.00
034440.8+320455	17.57	034443.0+321559	14.38	034445.4+320556	20.05
034440.9+321010	13.63	034443.2+320801	19.51	034445.5+320513	17.56
034440.9+321718	13.80	034443.2+320257	20.15	034445.5+320628	19.14
034440.9+320615	19.65	034443.2+321239	19.12	034445.5+321403	19.81
034440.9+321533	18.95	034443.3+320131	17.90	034445.5+320710	17.16
034441.0+320150	18.11	034443.3+320940	17.32	034445.6+321452	17.91
034441.0+320623	19.21	034443.4+320817	11.70	034445.6+321110	15.05
034441.1+320217	15.14	034443.4+321537	19.42	034445.7+321405	19.48
034441.1+320807	14.53	034443.5+320742	12.14	034445.7+321524	19.90
034441.1+320346	19.24	034443.5+321212	19.97	034445.8+320624	19.72
034441.1+321009	13.63	034443.6+321254	20.04	034445.8+320521	19.53
034441.2+320627	14.27	034443.7+320547	16.40	034445.9+320356	15.28
034441.2+320412	18.31	034443.7+320906	18.26	034446.0+320353	18.46
034441.2+320614	18.69	034443.7+321047	14.47	034446.0+321205	15.15
034441.2+321216	18.74	034443.7+321547	18.81	034446.2+321219	19.34
034441.3+320936	19.55	034443.8+321523	18.54	034446.2+320810	17.15
034441.3+320422	16.90	034443.8+320540	19.80	034446.2+320829	19.13
034441.3+320453	14.54	034443.8+321030	12.29	034446.2+321135	20.42
034441.3+321025	12.54	034443.8+321351	19.65	034446.2+320312	13.79
034441.4+321309	13.44	034443.8+321549	19.59	034446.3+320215	17.70
034441.6+321039	15.36	034443.8+321154	19.04	034446.3+321116	14.00
034441.6+321313	19.23	034443.8+321539	18.91	034446.3+321342	16.34
034441.6+320912	20.13	034443.9+320836	17.91	034446.3+321226	20.17
034441.7+320835	20.01	034444.0+320521	18.55	034446.4+320346	17.80
034441.7+321202	13.19	034444.0+320539	16.22	034446.4+321331	19.59
034441.7+320313	18.88	034444.1+320140	20.27	034446.5+321350	18.57
034441.8+320552	20.39	034444.2+321325	18.89	034446.6+320901	15.33
034441.8+321417	19.04	034444.2+320943	18.50	034446.7+320323	17.96
034441.9+320312	19.72	034444.2+320341	17.69	034446.7+320928	20.05
034441.9+320414	18.68	034444.2+320847	14.50	034446.7+321445	19.94
034442.0+320446	18.01	034444.3+321036	15.33	034446.8+320616	18.22
034442.0+320859	12.32	034444.4+320439	20.09	034446.8+320446	19.92
034442.1+320236	19.18	034444.4+321005	14.97	034446.8+320418	19.31
034442.1+320258	12.69	034444.5+320514	18.33	034446.8+321153	18.87
034442.1+320638	20.41	034444.6+320812	12.86	034446.9+320536	14.31
034442.1+320901	11.86	034444.6+321237	20.15	034446.9+320634	18.29
034442.3+320744	20.14	034444.6+320730	13.75	034447.3+320527	18.86
034442.3+321001	20.09	034444.6+320916	20.09	034447.4+320835	18.35
034442.3+321228	16.13	034444.7+320512	17.20	034447.4+321427	19.56
034442.3+321401	19.38	034444.7+320402	11.01	034447.4+321516	17.59
034442.3+321513	16.12	034444.8+321255	18.68	034447.4+320439	20.15
034442.5+321030	19.77	034444.8+320540	17.21	034447.4+321047	19.67
034442.6+321002	13.63	034444.8+321028	19.43	034447.5+321123	20.10
034442.6+320340	19.81	034444.8+321105	13.08	034447.6+320446	19.84

Table 1. continued.

IC348-J	*J* [mag]	IC348-J	*J* [mag]	IC348-J	*J* [mag]
034447.6+321714	16.46	034450.5+320800	20.24	034453.4+321110	18.92
034447.6+321055	13.51	034450.6+320615	19.48	034453.4+321539	20.31
034447.7+320353	17.64	034450.7+320521	19.66	034453.4+321550	18.83
034447.7+321255	19.72	034450.7+321718	15.89	034453.5+320617	18.37
034447.9+321325	20.06	034450.8+321414	18.32	034453.5+321652	19.55
034447.9+320256	20.32	034450.9+321629	17.87	034453.5+321356	17.57
034447.9+320404	19.15	034451.0+321609	12.36	034453.6+321404	19.97
034447.9+320951	18.80	034451.1+320649	20.13	034453.6+320343	17.72
034448.0+321140	18.95	034451.2+320359	19.18	034453.6+320858	14.83
034448.1+320737	19.95	034451.2+321327	19.90	034453.6+321557	20.03
034448.1+321500	18.68	034451.2+321504	14.05	034453.6+321721	20.49
034448.1+321522	17.02	034451.4+320946	17.22	034453.7+320652	13.19
034448.1+321627	20.17	034451.5+320751	18.76	034453.8+321118	19.61
034448.3+321226	17.57	034451.5+320429	16.92	034453.9+320615	20.13
034448.4+320711	20.31	034451.6+321213	20.50	034453.9+320436	20.37
034448.4+320859	18.73	034451.7+321402	20.42	034453.9+321024	19.45
034448.5+321527	11.40	034451.8+320346	19.96	034453.9+321045	20.22
034448.5+321518	20.53	034451.8+320917	18.42	034453.9+320913	19.20
034448.6+320530	20.02	034451.8+320950	15.60	034453.9+321349	18.83
034448.7+321703	20.18	034451.8+321118	17.55	034453.9+321508	18.86
034448.7+320140	19.59	034451.8+320835	19.63	034454.0+321723	18.52
034448.8+321322	13.24	034451.9+321336	20.17	034454.0+320230	19.28
034448.8+320419	17.11	034451.9+320521	20.31	034454.0+320931	19.77
034448.9+320733	20.29	034451.9+320628	18.37	034454.0+321524	19.04
034448.9+320407	19.33	034451.9+320957	17.88	034454.1+321653	20.03
034449.0+321626	19.58	034451.9+321319	18.18	034454.2+320427	18.05
034449.1+320847	19.83	034451.9+321635	15.27	034454.2+321117	19.94
034449.1+320505	20.18	034452.0+320617	20.27	034454.4+320613	18.93
034449.3+320949	18.46	034452.1+320446	13.89	034454.5+321015	18.95
034449.4+321504	18.68	034452.1+321006	19.48	034454.7+320440	19.35
034449.5+321020	16.33	034452.1+321028	18.37	034454.7+320611	20.17
034449.5+321217	16.53	034452.2+320512	19.24	034454.9+321345	19.94
034449.6+320911	13.22	034452.3+321022	19.59	034455.0+321210	10.43
034449.6+321129	18.98	034452.3+320717	20.02	034455.0+321447	19.87
034449.6+321645	11.17	034452.3+321127	17.41	034455.0+321006	16.98
034449.7+321407	19.64	034452.3+321455	20.07	034455.1+320557	19.98
034449.8+320941	19.00	034452.4+321337	19.32	034455.1+321154	17.90
034449.8+320334	13.18	034452.5+320710	17.17	034455.1+321438	19.38
034449.8+321731	20.45	034452.5+320741	16.28	034455.2+320151	19.79
034449.8+320844	18.66	034452.5+321634	19.03	034455.2+321008	20.46
034449.9+321608	18.81	034452.6+321006	19.06	034455.2+321213	14.32
034449.9+320614	18.01	034452.6+321008	17.68	034455.2+321503	18.11
034449.9+321706	18.06	034452.6+321032	19.31	034455.2+321520	18.91
034449.9+320841	17.19	034452.6+321331	19.97	034455.2+320656	19.86
034449.9+321602	17.09	034452.7+320202	20.19	034455.2+321506	18.50
034450.0+320345	12.51	034452.7+320654	20.10	034455.3+320541	17.89
034450.0+321117	15.31	034452.7+321703	19.70	034455.3+320912	18.25
034450.1+320747	19.26	034452.7+321708	19.45	034455.3+321502	14.78
034450.1+320843	17.70	034452.7+321017	17.13	034455.3+320729	16.32
034450.2+320635	18.86	034452.9+320942	17.75	034455.3+320934	13.47
034450.2+320714	18.17	034452.9+321705	18.14	034455.4+320516	15.47
034450.3+321351	18.78	034453.0+320507	20.32	034455.4+321351	16.92
034450.3+321635	19.17	034453.0+320655	19.64	034455.5+320524	18.38
034450.3+320345	19.13	034453.1+320518	15.91	034455.5+321414	16.88
034450.4+320356	20.53	034453.1+321219	20.22	034455.5+320123	20.12
034450.4+320515	20.12	034453.1+321311	19.83	034455.5+321307	17.12
034450.4+320754	19.16	034453.3+320430	18.99	034455.5+321346	19.06
034450.5+321209	18.02	034453.3+321133	19.87	034455.6+320919	11.87

Table 1. continued.

IC348-J	*J* [mag]	IC348-J	*J* [mag]	IC348-J	*J* [mag]
034455.7+321032	19.51	034457.8+321100	20.11	034500.8+321229	17.20
034455.7+320619	19.95	034457.9+320401	13.45	034500.8+321635	17.56
034455.8+320405	20.20	034457.9+320716	19.24	034500.9+320808	16.82
034455.8+321403	17.41	034458.0+321155	18.81	034500.9+320352	19.58
034455.8+320844	15.62	034458.0+321153	20.41	034501.0+320953	18.52
034455.8+321313	17.66	034458.0+320454	18.66	034501.0+320955	19.25
034455.9+321137	20.14	034458.1+321250	17.65	034501.0+321222	14.20
034455.9+320726	13.67	034458.2+320710	15.39	034501.0+321605	20.32
034456.0+321001	19.40	034458.2+321314	18.56	034501.1+321426	20.19
034456.0+321351	15.28	034458.2+320408	17.23	034501.1+320320	13.96
034456.1+320355	17.29	034458.2+321527	18.13	034501.1+320226	14.35
034456.1+320556	12.97	034458.3+321633	19.57	034501.2+321031	19.90
034456.1+320504	19.38	034458.4+320844	18.83	034501.3+320938	18.93
034456.1+320534	16.37	034458.4+320207	16.61	034501.3+320420	20.07
034456.1+320915	11.03	034458.6+320710	18.67	034501.3+321313	15.47
034456.2+320901	20.20	034458.8+320638	18.61	034501.4+321002	20.13
034456.2+321048	19.58	034458.8+320323	20.05	034501.5+320500	10.32
034456.3+320933	20.34	034458.8+321529	20.21	034501.5+320239	19.86
034456.3+321031	15.87	034459.0+320654	20.32	034501.5+321229	13.26
034456.3+321035	16.58	034459.0+320901	17.60	034501.5+321315	18.19
034456.4+320729	19.93	034459.0+320441	18.76	034501.5+321446	19.17
034456.4+321438	18.72	034459.0+320433	19.26	034501.5+321051	11.89
034456.4+321700	16.71	034459.0+321455	17.27	034501.6+321109	17.54
034456.4+321335	18.52	034459.1+320437	20.37	034501.6+321317	14.43
034456.4+320310	19.66	034459.1+321010	16.34	034501.6+320935	18.09
034456.5+320207	19.48	034459.1+321102	17.41	034501.7+320429	17.80
034456.5+320444	19.81	034459.1+321422	16.44	034501.7+320254	19.55
034456.5+320634	19.73	034459.2+320253	18.33	034501.8+321210	19.30
034456.6+321131	20.10	034459.3+320605	19.59	034501.8+321427	11.36
034456.7+321225	17.69	034459.3+320634	20.08	034501.8+321434	17.60
034456.8+321134	19.91	034459.4+320139	19.80	034501.8+320650	17.83
034456.8+321703	16.56	034459.4+320141	17.62	034501.8+320242	19.25
034456.8+320324	19.56	034459.4+320907	17.80	034502.0+320744	20.10
034456.8+320545	13.58	034459.4+320437	18.29	034502.1+321455	17.67
034456.9+320914	16.34	034459.4+321338	20.12	034502.1+321355	18.46
034456.9+320418	19.66	034459.5+321039	13.25	034502.3+320628	20.03
034457.0+320346	19.68	034459.6+321424	14.31	034502.3+321115	20.20
034457.1+320211	19.34	034459.6+320633	18.16	034502.3+320816	17.74
034457.1+321348	15.50	034459.7+321131	19.87	034502.3+321031	19.83
034457.2+321225	20.21	034459.8+320647	14.62	034502.4+320614	20.00
034457.2+320234	18.38	034459.9+321332	13.76	034502.4+321016	18.43
034457.2+321007	19.43	034459.9+320802	20.22	034502.5+320929	19.27
034457.3+320850	18.31	034459.9+320647	14.62	034502.5+321213	19.29
034457.3+320835	17.82	034459.9+320242	20.02	034502.6+320728	19.46
034457.4+320115	19.91	034500.1+321302	17.18	034502.6+321046	18.86
034457.4+320211	20.15	034500.1+320430	19.09	034502.6+321331	16.60
034457.4+320258	17.57	034500.2+320651	18.38	034502.6+320633	16.39
034457.5+320942	18.20	034500.2+321324	14.56	034502.7+321248	19.57
034457.5+321521	18.38	034500.3+321251	18.97	034502.7+321524	16.93
034457.5+320809	19.85	034500.4+321248	14.32	034502.7+321111	18.52
034457.6+320631	18.17	034500.5+320320	15.48	034502.8+320544	17.87
034457.6+321718	18.17	034500.5+321047	18.50	034502.8+320700	12.69
034457.6+320701	13.55	034500.5+321258	18.80	034502.8+321407	17.03
034457.6+321224	12.31	034500.5+320534	19.39	034502.9+320240	17.98
034457.7+320741	14.16	034500.5+320616	18.62	034502.9+320550	16.78
034457.7+320744	21.68	034500.5+321403	18.06	034502.9+321127	19.31
034457.7+320837	18.40	034500.6+320819	14.21	034502.9+321435	20.30
034457.8+320722	17.17	034500.7+321057	18.35	034503.0+320444	19.97

Table 1. continued.

IC348-J	*J* [mag]	IC348-J	*J* [mag]	IC348-J	*J* [mag]
034503.0+320122	17.73	034505.2+321628	17.25	034507.9+321639	19.22
034503.0+321125	15.97	034505.2+320954	12.99	034507.9+320532	19.34
034503.1+320617	15.87	034505.4+321216	15.32	034508.0+321637	20.23
034503.1+321252	17.85	034505.4+321227	19.70	034508.0+321551	19.74
034503.2+321421	19.93	034505.4+320420	17.61	034508.0+320354	19.29
034503.2+321150	18.16	034505.4+320308	14.38	034508.0+320400	10.28
034503.2+320405	11.94	034505.4+320920	20.46	034508.1+320412	18.71
034503.2+320714	17.17	034505.6+321130	19.12	034508.3+320429	18.91
034503.2+321529	18.57	034505.7+321417	15.24	034508.3+320915	17.89
034503.3+320706	20.41	034505.8+320308	11.76	034508.3+321307	19.15
034503.3+321311	20.35	034505.9+320119	18.89	034508.3+321523	20.09
034503.3+321417	18.26	034505.9+320826	16.03	034508.3+321336	18.17
034503.4+321549	20.24	034505.9+320238	17.24	034508.3+321004	19.79
034503.5+320858	18.96	034505.9+321426	19.89	034508.4+320701	16.16
034503.6+321435	19.72	034506.0+321216	17.65	034508.5+321149	20.06
034503.6+321213	17.25	034506.0+321555	19.68	034508.5+321031	18.47
034503.7+320659	19.83	034506.2+321556	18.54	034508.6+320234	17.54
034503.7+321043	18.83	034506.2+321304	18.50	034508.6+320606	20.05
034503.8+321320	19.47	034506.2+321400	19.04	034508.7+320924	20.13
034503.8+320237	17.77	034506.3+320552	17.22	034508.8+321357	19.27
034503.9+320812	17.81	034506.4+320709	16.03	034508.9+320244	20.09
034504.0+320251	19.85	034506.4+321704	18.51	034508.9+321546	18.17
034504.0+320656	19.46	034506.6+321019	18.12	034508.9+321147	19.83
034504.0+321007	19.67	034506.6+321533	19.16	034509.0+320547	19.56
034504.1+320259	20.43	034506.7+320834	17.32	034509.2+320114	16.26
034504.1+320540	19.92	034506.7+320930	13.71	034509.2+321615	19.83
034504.1+320504	16.45	034506.7+320535	16.07	034509.3+320805	20.24
034504.1+320813	18.28	034506.8+320755	18.16	034509.3+321221	20.16
034504.1+321104	17.24	034506.8+321253	18.48	034509.3+321519	16.19
034504.2+320603	18.20	034506.8+321350	19.75	034509.5+321303	15.98
034504.2+320739	18.72	034506.8+320539	18.51	034509.5+321111	18.59
034504.2+320746	16.83	034506.8+320541	16.95	034509.6+320902	20.09
034504.2+320559	16.50	034506.9+321242	15.10	034509.6+321302	17.87
034504.2+320332	19.71	034506.9+321614	20.12	034509.6+320828	18.55
034504.3+320844	19.87	034506.9+321352	17.15	034509.6+321338	13.98
034504.3+321324	18.06	034506.9+321506	18.34	034509.6+321603	11.95
034504.3+320305	14.06	034507.0+321702	18.69	034509.7+320158	19.47
034504.4+321522	20.36	034507.0+321245	20.48	034509.9+321335	14.13
034504.5+321027	19.67	034507.0+321403	16.40	034509.9+321525	19.84
034504.5+320306	16.95	034507.0+320232	19.27	034510.0+320533	19.66
034504.5+320133	17.01	034507.0+320607	19.61	034510.1+320449	14.91
034504.5+321425	19.95	034507.1+321530	19.91	034510.1+320945	17.38
034504.6+320830	19.39	034507.2+320651	16.58	034510.2+320919	20.03
034504.6+320504	19.25	034507.2+320748	20.08	034510.2+321304	16.97
034504.7+321501	13.42	034507.2+321310	19.86	034510.2+321457	20.16
034504.7+321638	13.41	034507.4+320242	19.56	034510.3+320858	17.83
034504.8+320400	19.77	034507.4+320712	20.28	034510.6+321427	17.95
034504.9+320211	19.99	034507.5+320909	14.63	034510.7+321318	18.60
034504.9+321219	19.83	034507.5+321435	18.35	034510.7+321410	20.17
034504.9+321607	19.03	034507.5+320855	17.43	034510.8+321300	20.21
034504.9+321018	19.28	034507.5+320952	19.80	034510.8+320330	20.20
034504.9+321722	19.60	034507.6+320514	16.35	034510.8+321626	17.97
034504.9+320732	16.86	034507.6+320222	19.49	034510.8+321305	18.91
034505.0+321655	20.08	034507.6+321027	10.14	034510.9+320753	18.84
034505.0+321442	18.41	034507.6+321040	19.69	034510.9+320743	18.11
034505.1+321132	19.51	034507.7+320818	19.51	034510.9+321340	18.50
034505.1+321655	17.17	034507.7+320338	14.07	034511.0+321700	15.79
034505.1+321635	19.75	034507.7+320836	18.33	034511.1+320852	14.33

Table 1. continued.

IC348-J	*J* [mag]	IC348-J	*J* [mag]	IC348-J	*J* [mag]
034511.2+321637	17.43	034514.0+320150	16.02	034516.6+321220	15.19
034511.2+320749	19.59	034514.0+321144	15.06	034516.7+321432	19.44
034511.3+321453	19.47	034514.0+320652	20.29	034516.8+320817	19.79
034511.3+321655	20.16	034514.0+321245	19.91	034516.8+321712	20.11
034511.3+321346	18.46	034514.0+321120	16.92	034516.9+321709	19.62
034511.4+320335	18.73	034514.1+320951	18.88	034516.9+320611	16.15
034511.4+320141	19.01	034514.1+321716	19.11	034516.9+320319	17.47
034511.4+320811	20.16	034514.2+320802	20.22	034516.9+321650	20.17
034511.5+321424	20.13	034514.3+321630	14.33	034517.0+321535	18.71
034511.6+321103	17.90	034514.3+320909	20.45	034517.0+320412	19.84
034511.7+321305	18.64	034514.4+321552	14.62	034517.0+321654	18.21
034511.8+320126	17.83	034514.4+320315	20.04	034517.1+320755	17.40
034511.9+321056	19.41	034514.4+320832	18.23	034517.2+321037	20.15
034511.9+321124	18.07	034514.4+321251	19.34	034517.3+320952	19.91
034512.0+320256	19.98	034514.5+320741	19.56	034517.3+321040	20.00
034512.0+321042	17.85	034514.7+321321	20.05	034517.3+321636	18.24
034512.1+321141	13.62	034514.8+320549	17.08	034517.4+321359	13.33
034512.1+320913	14.00	034514.8+321630	18.99	034517.4+321637	19.25
034512.1+321029	12.62	034514.8+321328	17.66	034517.4+321250	17.32
034512.2+320550	18.40	034514.8+321538	19.02	034517.5+321034	16.09
034512.2+321200	14.50	034514.9+321109	17.56	034517.5+320750	20.19
034512.2+321352	17.19	034515.0+321626	17.30	034517.6+320646	19.87
034512.4+321440	19.50	034515.1+320940	19.46	034517.6+321135	20.11
034512.5+321529	17.87	034515.1+321543	19.71	034517.6+320755	18.32
034512.5+320237	17.89	034515.1+321439	20.06	034517.7+320837	18.83
034512.6+321105	19.11	034515.2+321030	18.90	034517.8+321414	20.08
034512.6+320513	20.25	034515.2+321309	19.56	034517.8+320705	19.93
034512.6+321640	20.04	034515.2+321505	20.01	034517.8+320929	18.99
034512.6+320947	15.49	034515.3+321230	15.83	034517.8+321206	13.75
034512.6+321406	19.34	034515.4+321113	17.09	034517.9+321606	20.56
034512.7+321145	18.18	034515.4+321415	17.49	034517.9+321545	17.41
034512.7+321116	15.79	034515.6+320650	19.83	034517.9+321600	18.89
034512.7+321156	20.17	034515.7+320812	11.32	034518.0+321301	18.67
034512.8+320316	14.54	034515.7+321209	13.80	034518.0+321146	20.25
034512.8+320923	17.50	034515.7+320754	19.56	034518.1+321031	19.95
034512.8+321409	19.69	034515.8+321618	19.70	034518.1+321459	20.44
034512.9+320336	18.03	034515.8+320222	19.23	034518.1+321404	16.54
034512.9+321258	18.31	034515.8+321237	16.59	034518.2+320754	17.82
034513.1+320359	20.17	034515.8+320325	16.38	034518.2+320852	16.36
034513.1+320829	19.66	034515.9+320915	20.05	034518.2+321422	14.89
034513.2+321258	18.89	034516.0+321000	19.64	034518.2+320951	18.97
034513.2+321527	14.15	034516.0+321230	19.49	034518.2+320940	17.76
034513.4+320140	18.97	034516.0+320827	19.78	034518.2+320743	17.45
034513.4+321611	19.71	034516.0+321202	20.22	034518.3+320641	17.06
034513.4+321138	19.58	034516.1+320514	19.52	034518.3+320648	19.34
034513.5+320551	18.56	034516.1+321432	20.07	034518.3+321441	18.91
034513.5+320923	17.74	034516.1+320232	16.01	034518.4+320901	19.24
034513.5+321444	19.35	034516.1+321118	18.29	034518.4+321351	19.91
034513.6+320212	16.02	034516.2+321007	20.00	034518.4+320615	19.20
034513.6+321018	19.29	034516.2+321018	17.27	034518.5+321251	18.23
034513.6+320120	11.60	034516.2+321718	16.22	034518.6+320949	19.57
034513.6+321348	16.07	034516.2+320648	19.73	034518.7+320331	20.21
034513.7+320307	19.40	034516.3+320619	11.97	034518.7+321033	19.99
034513.8+321210	16.85	034516.4+321303	18.78	034518.8+321042	19.25
034513.8+321408	18.12	034516.4+321652	14.89	034518.8+321646	14.60
034513.9+320924	18.76	034516.4+321546	18.06	034518.9+320301	20.26
034513.9+321414	19.03	034516.5+320942	15.13	034519.2+320239	18.69